JIMMA UNIVERSITY

SCHOOL OF GRADUATE STUDIES

COLLEGE OF NATURAL SCIENCES

DEPARTMENT OF CHEMISTRY

M.Sc. THESIS

ON

Solanum tuberosum PEEL EXTRACT MEDIATED SYNTHESIS OF COPPER OXIDE NANOPARTICLE AND SILVER DOPED COPPER OXIDE NANOCOMPOSITE AND EVALUATION OF THEIR ANTIMICROBIAL, ANTIOXIDANT AND PHOTOCATALYTIC DEGRADATION OF METHYLENE BLUE

BY: BETELEHEM G/SILASIE

ADVISOR: GUTA GONFA (Ph.D)

CO-ADVISOR: GEBRU G/TSADIK (Ph.D)

DECEMBER, 2023

JIMMA, ETHIOPIA

Solanum tuberosum PEEL EXTRACT MEDIATED SYNTHESIS OF COPPER OXIDE NANOPARTICLE AND SILVER DOPED COPPER OXIDE NANOCOMPOSITE AND EVALUATION OF THEIR ANTIMICROBIAL, ANTIOXIDANT AND PHOTOCATALYTIC DEGRADATION OF METHYLENE BLUE DYE

THESIS SUBMITTED TO THE SCHOOL OF GRADUATE STUDIES JIMMA UNIVERSITY FOR PARTIAL FULFILLMENT OF THE REQUIREMENTS FOR THE DEGREE OF MASTER OF SCIENCE IN CHEMISTRY (INORGANIC)

BY: BETELEHEM G/SILASIE

ADVISOR: GUTA GONFA (Ph.D)

CO-ADVISOR: GEBRU G/TSADIK (Ph.D)

Graduate Thesis Ownership Agreement

This thesis is a property of Jimma University, an institution that awarded MSc Degree to the graduate student and funded its research cost fully or partly. The research work was accomplished under the close support and supervision of the assigned University's academic staff. It is therefore strictly forbidden to publish, modify, or communicate to or put at the disposal of third party the entire document or any part thereof without the common consent of the research supervisor(s) and the graduate student. Disregarding this agreement would lead to accountability according to the Jimma University's Research and Publication Misconduct Policy **Article 1.7** of the University's Document for "Guidelines and Procedures for Research, March 2012".

Name of the Graduate Student	Signature	Date
_____	_____	_____
Name (s) of the Research Supervisor (s)	Signature	Date
_____	_____	_____
_____	_____	_____
_____	_____	_____

Title of the Thesis:

Solanum tuberosum peel extract mediated synthesis of CuO NPs and Ag-CuO NCs and evaluation of their antimicrobial, antioxidant and photocatalytic degradation activities

Degree Awarded: **MSc**/PhD (Encircle one)

College of Natural Sciences, Jimma University

DECLARATION

I declare that the work described in this thesis is my original work under the supervision of my advisor Guta Gonfa (Ph.D) and Co-advisor Gebru Gebretsadik (Ph.D) at the Department of Chemistry, Jimma University for the degree of M.Sc. in Inorganic Chemistry. I also declare that the substance of this thesis has neither been submitted elsewhere nor is being currently submitted for any other degree. I further declare that the thesis embodies the results of my research or advanced studies and that it has been composed by me. Where appropriate I had acknowledged the work of others.

Name: Betelehem G/silase Signature_____

Place: Jimma University, Jimma

TABLE OF CONTENT

CONTENTS **PAGES**

LIST OF TABLES

LIST OF FIGURES

APPENDIX

LIST OF ABBREVIATIONS AND ACRONYMS

AMR	Antimicrobial resistance
DDW	Double distilled water
DPPH	2, 2-diphenyl-1-picrylhydrazyl radical
FT-IR	Fourier-transform infrared spectroscopy
MO NP	Metallic oxide nanoparticles
MNP	Metallic nanoparticle
MNC	Metal nanocomposite
MB	Methylene Blue
NP	Nanoparticle
NC	Nanocomposite
NM	Nanomaterial
ROS	Reactive oxygen species
SEM	Scanning electron microscopy
STPE	Solanum tuberosum peel extract
TEM	Transmission electron microscope
UV-Vis	Ultraviolet-visible
XRD	X-ray diffraction

ACKNOWLEDGEMENT

First and foremost, I would like to extend my great thank, appreciation and respect I have benefited significantly from people that I would like to acknowledge. Firstly, I am grateful to go to my hard-working advisors: Guta Gonfa (Ph.D) and co-advisor: Gebru Gebretsadik (Ph.D) for their great supervision and scientific input for different ideas on current research area, suggestions, comments, professional and technical guidance of this research.

Next my special appreciation and thanks goes to Bonga college of Education and my families for their support all direction. Then, I would like to thanks Jimma University College of natural sciences and department of chemistry for their fund and providing required materials to do my research.

Above all, I would like to express my deepest gratitude to almighty lord, Jesus Christ for his infinitive in helping throughout my life, the embodiment of wisdom who provides me health, strength, and accurate insight into reality for his divine intervention during my research work.

ABSTRACT

Since the prevalence of multi-drug resistance micro-organisms cause serious infectious disease to be greatest health challenges in worldwide which are treated by antibiotics. Antibiotic resistance leads to higher medical expenses, prolonged hospital stays, and increased mortality. In addition, oxidative stress results in excessive production of free radicals causes serious chronic disease like cancer, diabetes, stroke and heart disease. On the other side the unavailability of clean water prompted from industrial application of methylene blue dye is one of the significant burdens for human health and environment. In these regard, metal oxide nano-based drugs and nano catalyst are possible alternatives to overcome the aforementioned problems. There are distinct physical and chemical methods of synthesis of nanoparticle usually uses non-biodegradable reducing agent and toxic organic solvent. Herein, noble phytochemical mediated synthesis of silver doped copper oxide nanocomposite is a simple, cost effective, non-toxic, and eco-friendly than commonly used methods. As a result, this study was aimed to synthesize Ag-CuO NCs via facile and cost effective phytochemical assisted co-precipitation method by mixing of Cu $(NO_3)_2.3H_2O$ and $AgNO_3$, using *solanum tuberosum* peel extract as reducing agent. The synthesized NPs were characterized by UV−vis, FT-IR, XRD and SEM. The UV−vis analysis showed a red shift after silver doping, indicating a decrease in the optical band gap values from 2.96 to 2.64 eV. FT-IR spectroscopy analysis confirmed the involvement of phytochemicals in stabilization and reduction of the NCs. XRD studies showed the purity and crystalline structure of CuO NPs and Ag-CuO NCs with crystallite sizes of 15 and 18 nm respectively. SEM result shows a spherical and mixture of spherical with rod-like shape for NPs and NCs respectively. The Ag–CuO NCs demonstrated remarkable inhibitory activity against *S.aureus* (26±0.53 mm) and *E.coli* (25±0.56 mm) at 100 mg/mL. Ag–CuO NCs exhibited outstanding DPPH radical scavenging activity with a low IC_{50} value of 35.17μg/mL. Concerning the environmental applications, the 5% Ag–CuO NCs displayed efficient photocatalytic activity against MB dye degradation up to 97% with comparing to 88% of pure CuO NPs within 120 min. Furthermore, the findings of our investigation displayed 5%Ag–CuO NCs is remarkably effective for bioremediation and environmental applications.

Keywords: *Solanum tuberosum* peels extract, Doping, CuO NPs, Ag-CuO NCs, Antimicrobial Antioxidant, Photocatalytic degradation.

1. INTRODUCTION

1.1 Background of the study

Nowadays, microbial resistance against routinely administered antibiotics is a global dilemma arising due to the overuse and misuse of drugs[1]. Besides, poor quality of convectional antibiotics leads to higher medical expenses, longer hospital stays, and increased mortality. Moreover, antibiotic resistance has been reached to a critical level, invalidating the effectiveness of the most antimicrobial drugs now used in clinical settings. In fact, the WHO has triggered the alarm signal for the research of novel drug that can either kill or inhibit spread of antimicrobial resistant micro-organisms [2]. In this regards, research works based on the noble phytocapped synthesis of metal doped metal oxide NCs-based drugs are amongst the most influential, operative and could be projected as sustainable alternative to inhibit the growth or kill against wide range of clinically relevant antibiotic-resistant pathogenic strains [3].

Apart from microbial resistance, several free radicals resulted from oxidative stress were identified in many illness, including cancer, heart disease, diabetes, stroke, aging and cardiovascular disorder, which demolish the target molecule by extracting an electron to get stable [4]. Also, ROS and free radicals are produced in human bodies either through normal metabolic processes or from external sources such as exposure to sun light, ozone, cigarette smoking, air pollutants, and industrial chemicals [4]. However, these free radicals can be deactivated using antioxidants, before they attack body cells and manifest a disease. As result, phytocapped Ag doped CuO NCs are particularly renowned for effectively scavenging of free radicals containing oxygen groups compared to other antioxidants supplements [5].

On the other hand, the shortage of clean water in society has recently been linked to water pollution caused by untreated MB dye effluents from industry [6]. This is common in developing countries where high volume of wastewater discharged into the physical environment without effective and efficient treatment[7].In order to remove toxic organic pollutants, several convectional waste water treatment techniques, like adsorption, reverse osmosis, Flocculation, coagulation, evaporation and electro precipitation were used[8]. However, the above mentioned methods have their own limitations such as incomplete removal of the pollutants, high energy consumption, high cost, require sensitive equipment, and production of secondary pollutants or

large amount of sludge that require further disposal. Therefore, metal oxide semiconductor nanomaterial based photocatalytic degradation is a suitable choice for the degradation because the process is fast, simple, efficient, inability to generate secondary pollutant and environmentally friendly [9]. In this regards, phytocapped Ag-CuO nanocatalyst could be effective photocatalyst under sun light for degradation of MB dye as compared to undoped CuO NPs due to Ag ion doping reduce bandgap energy for production high amount of ROS and shifting of bandgap towards red shift for better absorption for degradation.

The wide scope of technological applications of nanomaterials(NMs) has made nanotechnology as one of the most promising research area and a borderline between nanoscience and material science [10]. NMs with unique small size ranges from 1-100 nm and high surface area qualify them more fascinating for various applications including in medical and environmental remediation [11]. Metallic oxide based NPs such as Fe_2O_3, TiO_2, MnO, CuO, NiO, ZnO have fascinated scientist for over a century and are now heavily utilized in biomedical sciences and engineering. Recently CuO NPs have gotten a lot of attention because it is the simplest, low cost, non-toxic and abundance [12]. However, its limited visible light harvesting and unwanted fast recombination of photogenerated e^- and h^+ makes it inefficient for photocatalytic reaction. Consequently, doping with metal cation such as lanthanum, platinum, silver, gold have enhanced catalytic by reducing e^- and h^+ recombination rate and shifting the band gap towards visible region of spectrum for better absorption [13] .

Numerous physical and chemical methods were employed for synthesis of CuO NPs and Ag doped CuO NCs usually uses non-biodegradable stabilizing agents, organic solvents and toxic reducing agents. In order to minimize aforementioned challenges, phytochemical mediated synthesis of NPs using plant extracts has drawn attention for being an environmentally and eco-friendly safe choice [14]. *Solanum tuberosum L.* belongs to family *Solanaceae* locally known as Dinchi in Amharic and Dincha in affaann Oromo is a globally important crop plant producing high yields of nutritionally valuable food in the form of tubers [15].Traditionally potato peel used to treat acne, reduce excessive oil and even to get rid of dark circles and moisturizer; used as face mask. Due to, its traditional medicinal value and its rich in bioactive compounds like phenolic, alkaloids, tannins and flavonoids, which play a crucial role in metal reduction ,

capping and stabilizing process during the synthesis of NCs [16]. Utilization of these wastes in various areas could help in mitigating environmental pollution.

With this in mind, previous works on green synthesis of Ag-CuO NCs using leaf extract of *Mimosa pigra* [17], *Bergenia ciliate* [18],*Malus Domestica* [19], Murraya koenigii and Zingiber officinale [20] were reported. However, those plants extracts were either limited only to physico-chemical studies or focus only on antibacterial activity or photocatalytic activity. None of the above-cited articles reported the antimicrobial, antioxidant and photocatalytic degradation of MB dye under solar irradiation yet not investigated. To the best of our knowledge, this is the first report on synthesis of CuO NPs and Ag-CuO NCs using *Solanum tuberosum* peel extract and physicochemical properties were studied through UV-vis, XRD, FT-IR and SEM. Thus, this was planned to explore the dynamic multifunctional nature of CuO NPs and Ag-CuO NCs by performing antimicrobial activities against (GPB, GNB and *C.albinica*), antioxidant activity towards DPPH and Photocatalytic activity towards degradation of MB dye by sunlight.

The selection of *Solanum tuberosum* peel extract as a green source for the synthesis of CuO NPs and Ag-CuO NCs was purely based on its easy availability, medicinal value and phytochemical composition based on the literature [16]. The antimicrobial, antioxidant and photocatalytic performance under solar light of the synthesized CuO NPs and Ag-CuO NCs was evaluated practically. It was observed that 5% Ag doped CuO NCs have exhibited best performance in antimicrobial, antioxidant and photocatalytic degradation of MB dye compared to undoped pure CuO NPs.

1.2 Statement of the problem

Increasing of antimicrobial resistance due to inappropriate use of drugs, highly mutative capacity and rapid morphological change of pathogenic micro-organisms is one of the major problems facing the modern scientific community [21]. A part from microbial resistance several free radicals and ROS were generated and cause chronic and degenerative diseases such as cancer, stroke, diabetes and heart disease by causing oxidative stress. Furthermore, unavailability of safe drinking water sources is a main concern in many countries around the world especially in developing country. Moreover, the pollution of water bodies by untreated MB dye effluents

discharged from industries has been recently associated with the shortage of clean water in the society and risk for aquatic organism [22].

Nature has provided ways and insights into the simple and green synthesis of NPs using plant extract and micro-organisms. However, the synthesis of NMs using microorganisms are tedious and find special care for example, storing microorganisms, as well as their isolation, culturing, and sampling; all of these steps are complicated. As a result, Phytocapped synthesis of NPs have attracted attention which is simple, cost effective, bio-compatible, high resultant yield production, stable NPs formation and eco-friendly safest choice [14]. Previously Ag-CuO NCs were synthesized from leaf extract of *Mimosa pigra* [17], *Bergenia ciliate* [18],*Malus Domestica* [19], Murraya koenigii and Zingiber officinale [20]. None of these reports evaluate its antimicrobial, antioxidant and photocatalytic degradation of MB and there was no research reported yet on *Solanum tuberosum* peel extract mediated Ag doped CuO NCs. In this manner, to fill the gap there could be widely available used waste, cheap, phytochemical rich, effective, economically viable and broadly applicable Ag doped CuO NCs could be synthesized using *Solanum tuberosum* peel extract. Thus, this research focused to investigate effect of doping Ag to a functional material CuO NPs on its antimicrobial, antioxidant and photocatalytic degradation of MB dye using phytochemical rich *Solanum tuberosum* peel extract. Thus, the findings of this study were answered the following questions:

- Does *Solanum tuberosum* peel extract have phytochemicals used for reducing, stabilizing and capping agent for CuO NPs and Ag-CuO NCs?
- Do CuO Nps and Ag doped CuO NCs are effectively synthesized by using STPE?
- Does Ag doping enhance the activities of antimicrobial, radical scavenging potential and photocatalytic degradation of MB dyes under solar irradiation activities?

1.3. Objective of the study

1.3.1. General objective

Main objective of the study is to synthesize CuO NPs and Ag doped CuO NCs using *solanum tuberosum* peel and evaluates their antimicrobial, antioxidant and photocatalytic degradation Methylene Blue.

1.3.2 Specific objectives

- To extract and screen phytochemicals found in STP using different reagents.
- To synthesize CuO NPs and Ag doped CuO NCs by using STPE as capping agent.
- To characterize CuO NPs and Ag -CuO NCs by using Uv-vis, FT-IR, SEM and XRD.
- To evaluate antimicrobial, antioxidant and photocatalytic activities of CuO NPs and Ag-CuO NCs towards degradation of MB dye under solar irradiation.

1.4 Significance of the study

Phytochemical mediated of metallic oxide NCs has recently become popular alternative over chemical and physical methods because of its simplicity, lower cost, relatively higher reproducibility and environmentally eco-friendly nature. In general, plants produce more stable NPs and it is straightforward to scale up for commercial application. Particularly Ag doped metal oxides NPs have charmed a lot of attention in photocatalytic, antioxidant and antimicrobial activities.The unique advantage is that silver ions have a relatively low toxicity to human cells while adversely affecting bacteria and fungi by interacting with bacterial cell membranes inhibiting reproduction of harmful micro-organisms[21].This study was expected to have its own contribution on the phytocapped synthesis of the NPs using widely used cheap waste extract and one alternative approach of synthesizing of high quality Ag doped with low cost Cu metal salt in greener method. As result the synthesis of Ag-CuO NCs by Chemical methods using toxic chemicals as reducing agent and non-biodegradable stabilizing agent was replaced by phytochemical mediated synthesis which is environmentally and eco-friendly nature using STPE as reducing and stabilizing agent which is biodegradable. Thus, this research study focused on STPE mediated synthesis of CuO NPs and Ag-CuO NCs for antimicrobial, antioxidant and photocatalytic degradation of MB dye under solar irradiation. Thus, the significance of these studies was;

1. Value adds on biomass (waste) mediated synthesis of NPs in circular economy.
2. It may be served as baseline to use Ag-CuO NCs for bioremediation for future applications in formulating the Ag-Cu based drug for human life-threatening from infectious diseases.
3. The applications of the STPE mediated Ag-CuO NCs may be scaled up by concerned stakeholders for practical applications widely.
4. Output of this research may motivate other researchers to study more on this area and used as reference.

2. REVIEW OF RELATED LITRATURE

2.1 Infectious disease and its remediation's

Infectious diseases are a set of illness or disorders caused by pathogenic microbes (bacteria, viruses, fungi, protozoa, parasites) that directly affect human health. In recent times, infectious diseases have become a great burden on the world economy as well as on public health. Various health issues including cholera, hepatitis B, hepatitis C, athlete's foot, tuberculosis, HIV, Covid-19, typhoid fever, Ebola, tonsils and monkey pox shown in (figure 1) are generally caused by microbes which cause death to millions of people around the world commonly in developing country especially in Africa. An estimated 2.8 million cholera cases and 91 000 deaths occur annually in cholera endemic countries [23]. A different study reported from various regions about the cholera outbreak showed that the total cases ranged between 25 to 36,154 cholera cases and around 246 deaths in Ethiopia were reported [24].

However, for the treatment of these infections, antibiotics are often the first choice. But microbes' growing resistance against these antibiotics coupled with the abuse of drug, highly mutative capacity and rapid morphological changes may lead to microbial resistance[25]. Moreover, inappropriate and irrational use of antibiotic provides favorable conditions for infectious disease emergence and re-emergence, often causing new pandemics [26]. To overcome the resistance developed by microbes, nanoparticle-based treatment presents a very promising approach. It has been noted that unique small size and high surface area to volume ratio of NMs makes them superior in treatment of different infectious disease. Therefore, research work on phytocapped Ag doped CuO NCs - based drug could be projected as sustainable alternative to fight against wide range of antimicrobial resistance microbes.

Figure 1.Infectious disease caused by micro-organisms (bacteria, virus and fungi) [29]

2.2 Oxidative Stress and Antioxidants

Oxidative stress is a manifestation of the imbalance between oxidants and antioxidant in biological system. The imbalance occurs as a result of the excess level of reactive oxygen species (ROS/ RNS) or improper functioning of the antioxidant system [4]. The body generates free radicals in response to environmental insults, such as tobacco smoke, ultraviolet rays, and air pollution, but they are also a natural byproduct of normal processes in cells. And also modern lifestyle associated with processed food, exposure to a wide range of chemicals and lack of exercise plays an important role in oxidative stress induction [4]. However, at high concentrations free radicals can be hazardous to the body and damage all major components of cells, including DNA, proteins, and cell membranes cause oxidative stress. Recent studies have shown that the abnormal expression of free radicals often leads to diseases such as: cancer, diabetes, stroke, aging and many other diseases leads to death [27].

Under sustainable redox conditions, the generation of ROS must be balanced by the antioxidant power of ROS scavengers. Antioxidants have become a vital part of our lives today. It is synthetic or natural substances added to products to prevent or delay their deterioration by action of oxygen in air [28]. All biological systems have antioxidant defense mechanism that protects against oxidative damages and repairs enzymes to remove damaged molecules. Many of the natural antioxidants of interest are of plant origin and belong to the phenolic and polyphenolic class of compounds as well as carotenoids and antioxidant vitamins, among others. However, this natural antioxidant mechanism can be inefficient; hence dietary intake of antioxidant compounds is important. Consequently, Phytocapped metal oxide NPs facilitate chemical stability of the ROS in physiological conditions [29].

2.2 Water pollution by synthetic dyes

There's nothing more essential to life on earth than water. People are struggling to access the quantity and quality of water they need for drinking, cooking, bathing, hand washing, and growing their food. Globally, 700 million people have no access to clean drinking water and half of them are located in Sub Saharan Africa, especially in Ethiopia [30]. Water pollution is one of the major and most urgent problems of the modern world. Due to the rapid industrialization, the use of coloring chemicals like dyes also increases day by day. Various industries like textile, leather,

food, paper, cosmetics and pharmaceutical are using variety of synthetic dyes [31]. The large-scale production and extensive application of synthetic dyes can cause considerable environmental pollution shown in figure (2), especially water pollution making it a serious public concern.

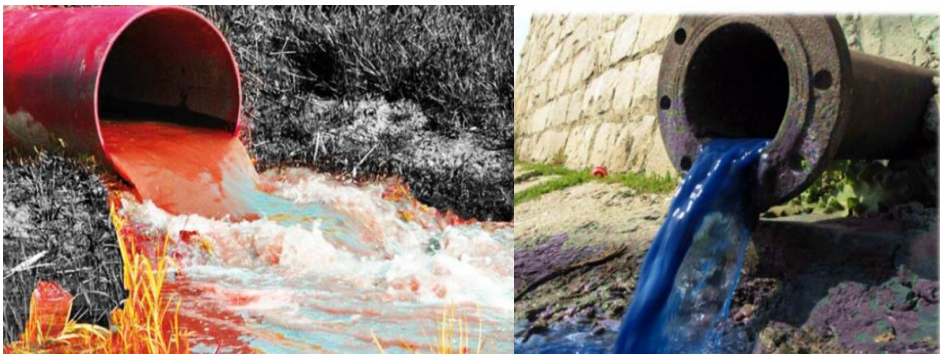

Figure 2 .Water pollution by different dyes effluents discharged from industries [34].

Among synthetic organic dyes, methylene blue (MB) dye is widely used in dyeing, tannery, plastic, cosmetics, food, leather, textile, paper and medicinal industries to add color to products. MB are reported to cause allergic dermatitis, skin irritation, cancer, and mutations [32] or on inhalation, it can give rise to short-term rapid or difficult breathing, while ingestion through the mouth produces a burning sensation and may cause nausea, vomiting, profuse sweating, mental confusion, and methemoglobinemia [33]. Therefore, MB dye containing wastewater must be treated and detoxified adequately before its final discharge into the environment. Conventional treatment methods are capable of color removal of MB dye from waste wastewater but are incapable of complete mineralization. Thus, metal oxide NMs based photocatalytic degradation of MB under solar irradiation is preferable due to its cost effectiveness, fast, nontoxic waste product and recyclability.

2.3 Nanomaterials and Metallic Oxide Nanoparticles

Nanomaterials are a materials possessing, at minimum one external dimension measuring 1-100 nm [32] . As the size is reduced to the nanometric scale, the exposed surface area increases and this favors the greater interaction between nearby atoms and molecules, giving rise to various interactions, attractions and repulsions. It cause surface, electronic and quantum effects that affect to the optical, electric and magnetic behaviors of the materials different from their bulk counterparts [33]. Metal oxide based NPs have fascinated scientist for over a century and are now heavily utilized in biomedical sciences and engineering. CuO NPs is one of the metallic oxide

multifunctional NP with useful physical properties applied in biomedicine, electron chemical effects, antimicrobial studies, fungicides, algaecides ,solar power generation and catalytic causes [34]. It is a promising p-type material with physiochemical properties strongly dependent upon its morphology and size. Cu is a relatively low-cost metal that is more cost-effective than Au and Ag. According to the United States Environmental Protection Agency, Cu and Ag has been recognized as an antimicrobial material that displays enhanced antimicrobial activity towards wide range of pathogenic micro-organisms [35].

2.4.Methods of synthesis of Metallic Oxide NPs

There are two prominent approaches for the synthesis of NMs, these are top- down approach and bottom–up approach [36] .

Top-down approach involves the breaking down of the bulk material into nanosized structures or particles shown in (figure 3a). Top-down synthesis (physical method) techniques consists in the manufacture of nanomaterials from larger-scale materials that are reduced to reach the nanometric scale. This method offers reliability and complexity in the devices, but it has associated high energy costs, greater imperfection on the surface and pollution problems.

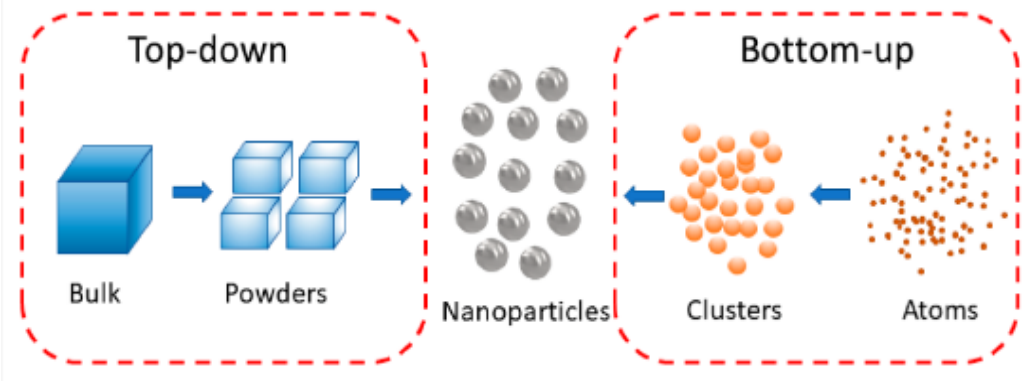

Figure 3.(a).Top-down and (b) bottom-up synthesis approach of NMs.

Bottom-up approach refers to the buildup of a material from the bottom: atom-by-atom, molecule-by-molecule, or cluster-by cluster shown in (figure 3 b). Many of these techniques (chemical and biosynthesis method) are still under development or are just beginning to be used for commercial production of nanopowders.

The most popular convectional chemical methods used to synthesize CuO NPs such as chemical precipitation, Co-precipitation, Sol-gel, hydrothermal and microwave-assisted methods are discussed below [37]. Chemical precipitation method are the common approach for synthesizing CuO NPs involves the precipitation of copper salts, such as copper sulfate or copper nitrate, with a suitable base, like sodium hydroxide or ammonia. The resulting precipitate is then calcined to form CuO NPs. Co-precipitation is very simple and efficient method for fabrication of CuO NPs. In this method, metal precipitates in the form of hydroxide from a salt precursor in the presence of a base in a solvent. In sol-gel method copper salt is dissolved in a suitable solvent and mixed with a gel-forming agent, such as tetraethyl orthosilicate. The gel is aged, dried, and calcined to yield CuO NPs. In hydrothermal method the process involves reacting copper salts with a suitable base under high temperature and pressure conditions in a sealed autoclave. The hydrothermal conditions promote the formation of CuO NPs. In microwave-assisted synthetic approach, copper salts are mixed with a base and heated in a microwave reactor. The rapid heating and uniform distribution of microwave energy facilitates the formation of CuO NPs.

In general, chemical and physical methods have the reputation of being expensive and poorly accessible to all scientists across the world, especially in developing countries. The reducing or capping agents are toxic, non-biodegradable and expensive. However, biosynthesis of NPs involves the synthesis of NPs by using plant extract and microorganisms. The synthesis of NMs using microorganisms are tedious and find special care for example, storing microorganisms, as well as their isolation, culturing, and sampling; all of these steps are complicated. On the other hand, phytonanotechnology has shown a new field for the synthesis of NPs which is eco-friendly, simple, cost effective, scalability, bio-compatibility, high resultant yield, highly stable NPs formation and synthesis via universal solvent (water). It uses different parts of plants for synthesis of NPs, such as root, fruit, stem, seed, peel (skin) and leaf.

2.4.1. Mechanisms of synthesis of NPs using plant extract.

The exact mechanisms for synthesis of NPs using plant remain to be elucidated. It has been illustrated that the secondary metabolites of plants are answerable for the reduction of metal ions into metal zerovalent atoms[38]. The secondary metabolites of plants, including alkaloids, flavonoids, polyphenols, and terpenoids act as a chelators to metal ions and reduce them into zero-valent states. Mostly the OH group of polyphenols and flavonoids develop coordination

with metal ions. In general, mechanism of plant extract mediated synthesis of NMs and NCs consists of three stages ;which includes activation stage, nucleation and growth stage [39]. The activation stage involves the reduction of metal ions and reduced metal atoms undergo nucleation; however, in the growth stage, spontaneous coalescence of small adjacent NPs into larger sized NPs and NCs took place. This stage is accompanied by increase in the thermodynamic stability of the NPs and NCs or a process known as Ostwald ripening shown in (figure 4). It is the termination stage in which the final shape of NPs and NCs are formed.

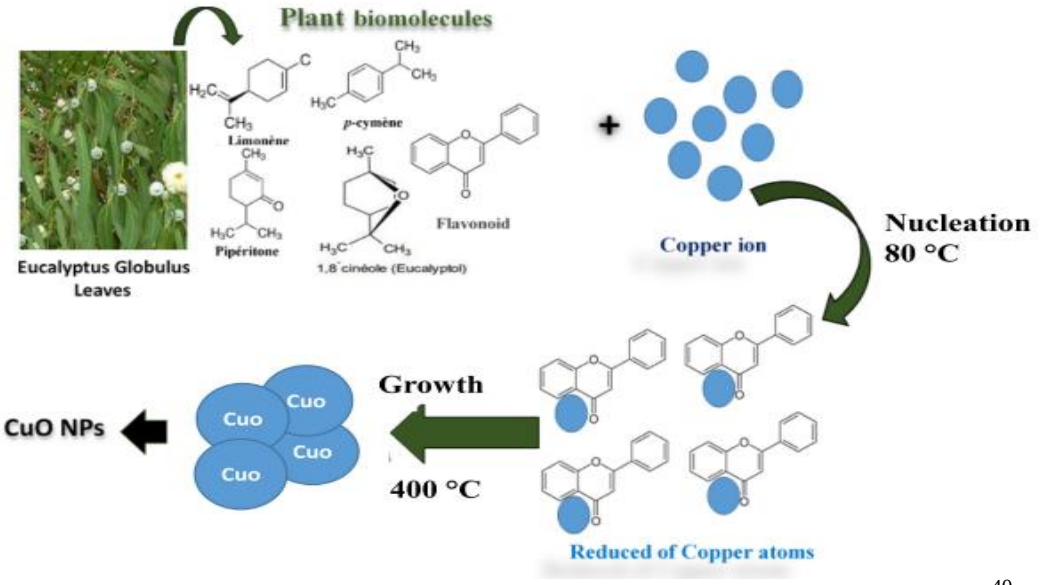

Figure 4 .Mechanism of MONP formation by plant extract mediated green synthesis [40] .

Ag-CuO NCs synthesis by using plant extract has benefits over other biological synthesis methods, such as microorganisms. In fact, the rate of metal nanocomposite synthesis with the help of plant extract is more persistent, significantly faster, and extremely mono-dispersive in respect to microorganism [41]. Ag-CuO NCs were previously successfully synthesized using leaf extract of *Mimosa pigra* [17], *Bergenia ciliate* [18],*Malus Domestica* [19], *Murraya koenigii* and *Zingiber officinale* [20] extract. The presence of various active biomolecules in the plant extract plays an important role in the reduction, capping and stabilization of metal ions in the solution by producing electrons.

2.5. *Solanum tuberosum* Peel eextracts and its phytochemical constituents

Solanum tuberosum L. (Solanaceae) known as potatoes is a globally important crop plant producing high yields of nutritionally valuable food shown in (figure 5) in the form of tubers [15].

Potato peel waste is the major waste from the potato processing industry and a potential source of functional and bioactive compounds, including dietary fiber, vitamins and minerals [42]. Potato peel also has haggard attention as a natural antioxidant in food system and antimicrobial due to its high content of polyphenols, which was reported to be 10 times higher than their levels in the flesh accounting for approximately 50 % of all polyphenols in potato tuber [43] .

Figure 5.Potato plant

With ever increased food processing in the new millennia, production of agro-industrial waste has been increased tremendously. Environmental pollution because of improper waste management is an alarming challenge for developing countries to meet the millennium development goals. For this reason, green chemistry is the need of today and light of future which gives a precious idea for the scientifically based environmental protection[44].

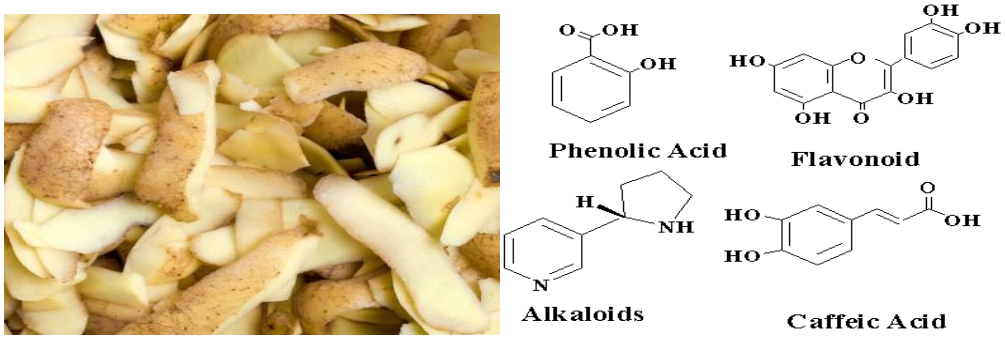

Figure 6.Potatoes Peel and its phytochemical components [50]

The results of the different preliminary phytochemical screening tests using water and ethanol solvent showed the presence of bioactive compounds like alkaloids, saponins, flavonoids, terpenoids, total phenols and tannins [45];shown above (in figure 6). Therefore, this cheap and

ever available waste can be considered as an excellent candidate for reducing, capping and stabilizing agent for MNPs.

2.7 Applications of silver doped copper oxide Nanoparticle

Antimicrobial activity

The smaller size and large surface area to volume ratio of nanoparticles made them a unique delivery and antimicrobial agents in many respect [46]. The size of NPs play a major role in biomedical activities; smaller NPs have more biological activity because of their high surface area bound on cell surface. Moreover, microbial cell wall penetration causes generation of reactive oxygen species which are capable of causing damage to cells through various processes. One of the most prominent of which is the interaction of protein thiol with hydroxyl radicals and superoxide, which deactivates membrane receptors damaged DNA and proteins, loss of cellular integrity are the underlying mechanisms that cause inhibition for bacteria and likewise fungi shown in (figure 7) [19]. According to El-Sayyad *et al*,[47] doped metal oxides are more effective in antimicrobial activities in both gram positive and gram negative bacteria and fungi; combinations of two individual metals may be more efficient than undoped metal oxide due to its reduced bandgap produced concentrated amount of ROS cause cell dysfunction in on microbial cell [48].

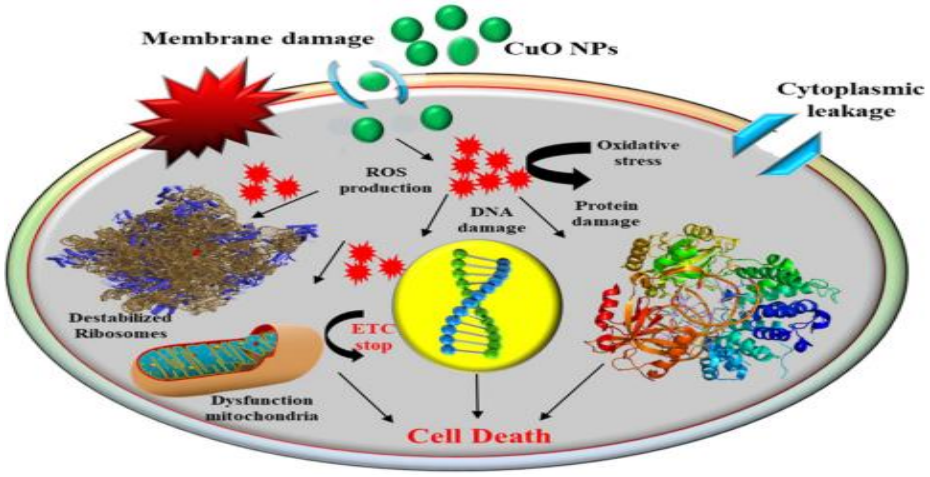

Figure 7.Mechanism of antimicrobial activity of NPs [21].

Antioxidant activity

Antioxidants have become a vital part of our lives today. Biosynthesized Metal doped metal oxide represent one of the most promising properties in the research for improved antioxidant

activity due to their small size and bioactive surface [5]. DPPH free radical scavenging is widely used stable nitrogen centered radical and accepted mechanism for screening the antioxidant activities of MO NPs synthesized from plant extract**.** The abundance of bioactive compounds on the surface of Nps is strongly correlated with donating of electron to reduce DPPH free radicals.Furthermore, DPPH free radicals have been found to be scavenged by several plant extracts consisting of a variety of polyphenols, flavonoids, alkaloids and so forth. It's mainly due to their redox properties which play an important role in scavenging and neutralizing free radicals. As noted previously, antioxidants react with DPPH• stable radicals via a combined hydrogen atom transfer (HAT) and single electron transfer (SET) mechanism [49].The free radical in the hydrogen atom transfer mechanisms intercepts one hydrogen atom from an antioxidant, and the antioxidant becomes a radical. On the other side, single electron transfer reaction is realized by the one electron transfer from the nucleophile to the substrate with the formation of a radical intermediate, which can be involved in the further process, as shown in (figure 8)**.** Then deep purple color of DPPH will be lost after it reduced to its non-radical form by antioxidants becomes light yellow colored Diphenyl picryl hydrazine and absorbs wavelength at 517 nm.

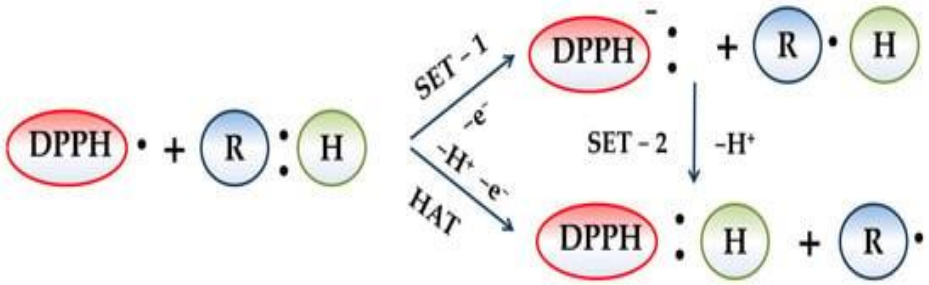

Figure 8.Mechanism of the DPPH radical scavenging with antioxidants 55

.

2.8 Photocatalytic degradation of MB dye

UV-light /sunlight-driven photo-catalysis is the most promising way for successfully removing organic pollutants without producing any harmful intermediates shown in (Equation 1). In this process, a photochemical reaction takes place on the surface of metal oxide semiconductors by involving two reactions - oxidation and reduction that occur simultaneously. Briefly, solar light is absorbed by the photocatalysts to generate pairs of electrons and holes when the light possesses enough photon energy which is more than or equal to the band gap energy of the photocatalyst. The generated e^- and h^+ pairs migrate to the surface of the photocatalyst to

undergo a redox reaction. However, a lot of these holes and electron pairs recombine to dissipate energies in the form of light and heat. To minimize recombination of photoinduced electron their must should dopant metal ion to trap electron. The unrecombined electrons are excited to the conduction band of the photocatalyst while the holes in the valence band of the photocatalyst attacks the methylene blue dye and some of the hole also react with water to generate hydroxyl radicals which in-turn strongly oxidize the MB dye. The excited electrons on the other hand further attack the oxygen to form superoxide anion radicals which also degrade the methylene blue dye in the presence of photocatalyst and light into carbon dioxide, water and other less toxic or non-toxic substances shown in (figure 9). The efficiency of the photocatalysis depends on the light intensity and the type of photocatalyst used (equation 1).

Photocatalyst + hν → (CB) e− + (VB) h^+

Atmospheric O_2 + (CB) e− → Super Oxide Anion (O_2*)

H_2O + (VB) h^+ → H^+ + Hydroxyl radical (OH·)

·OH/ O_2* + Organic dye (MB) → By-products (CO_2 + H_2O) ……..*(Equation 1)*

Doped metal oxide NPs has performed better photocatalytic than the un-doped metal oxide [50]. In fact, the performance was related to the amount of metal dopant that was present in the photocatalyst and by attributing effect to reduction in the band gap of the doped photocatalysts. In doping processes, the photo generated charge carriers recombination rate is usually decreased and less energetic radiation can be absorbed and exploited thanks to the defect states created in the band gap or to the introduction of energy levels in it.

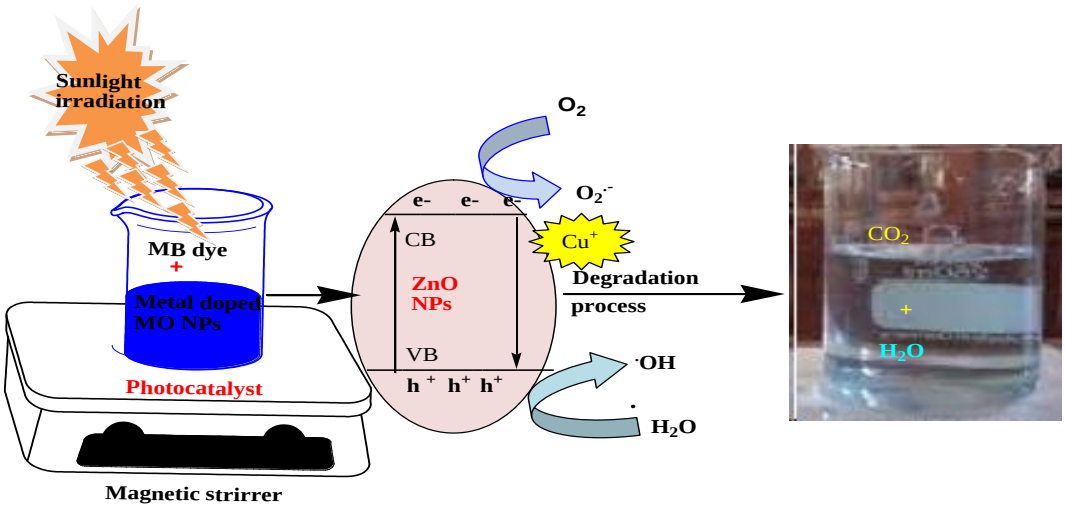

Figure 9.Photocatalytic degradation of MB dye by Cu doped ZnO NCs [57]

2.6. Physicochemical characterization of nanomaterials

Various techniques have been developed to characterize the size, shape, crystal structure, and chemical composition, optical, magnetic, and mechanical properties of NMs. Among these techniques, Uv-vis, FT-IR, SEM and XRD have been widely used to investigate the properties of synthesized NMs [51].

2.5.1 Ultra violet and visible (Uv-vis) spectroscopy

UV-vis spectroscopy is a relatively easy and low-cost characterization method that is often used for the study of nanomaterial's in aqueous solution by analyzing the unique optical properties and optical band gap which depends on the size of the NMs between 200 nm to 800 nm. It measures the intensity of light reflected from a sample and compares it to the intensity of light reflected from a reference material [52].

2.5.2 Fourier transform infrared (FT-IR) spectroscopy

It is a hugely popular technique today, due to its unique combination of sensitivity, flexibility, specificity and robustness.The FT-IR spectrometer simultaneously collects high-resolution information over a wide spectral range between 4000 and 400 cm^{-1}. Each molecule has a spectrum fingerprint that makes it unique and allows it to be distinguished from other molecules.It provides information about surface composition of functional groups of different phytochemicals which are responsible for reducing, stabilizing and capping agents [53].

2.5.3 Scanning electron microscopy (SEM)

A SEM is one of the common methods for imaging the microstructure and morphology of the materials.The electrons interact with atoms in the sample, producing various signals that contain information about morphologies and size distributions of NPs and NCs [54].

2.5.4. X-ray powder diffraction (XRD)

X-ray diffraction (XRD) technique is used to notice the structural properties of materials and give information like crystal structure/phase, lattice parameters, crystallite size, the orientation of single and polycrystals, defects and strains. [55].

3. MATERIALS AND METHOD

3.1.1 The Study Area and Period

The study was carried out at Jimma University main campus, Inorganic chemistry research laboratory 346 Km away from Addis Ababa, Ethiopia from March to July 2023.The FT-IR ,XRD and SEM characterization were done at Jimma University Institute of Technology and Adama Science and Technology Institute respectively.

3.1.2 Chemicals and reagents

Copper (II) nitrate trihydrate (Cu $(NO_3)_2.3H_2O$)~99%, Silver nitrate($AgNO_3$, 99.98%), Ferric chloride (anhydrated) ($FeCl_3$)~99%, Ascorbic acid ($C_6H_8O_6$ ~99%), Sodium hydroxide (NaOH), ~99%, Dilute hydrochloric acid (HCl)~99%, DPPH (99.95%), methylene blue ($C_{16}H_{18}ClN_3S$) ~99%,Dimethyl sulfoxide (DMSO) ~99%, Absolute Ethanol (99%) and Double-distilled water was used as solvent throughout the experiment. All chemicals were analytical grade and used without further purification.

3.1.3 Apparatus and equipment's

Digital balance, oven, Magnetic stirrer with hot plate, Micropipette (10-100µL), mortar and pestel Crucibles, Watch, Cuvettes, Centrifuge, Refrigerator Whatman No.1 Filter paper, Aluminum foil and pH meter were used for the study.

3.1.4 Scientific Instruments

Absorption spectrums were recorded with the Ultraviolet-Visible (UV-Vis) spectroscopy (Analytic Jena and UV-Jenway6705). Fourier transform infrared (FT-IR) spectrometry (65 FTIR Perkin Elmer) was used to identify the functional groups. The morphology of the sample was studied by scanning electron microscopy (SEM) (JCM-6000Plus) and X-ray diffraction (XRD) (XPERT PRO Machine) was used to analyze the crystallite nature and size of the sample.

3.2. Sample collection and Preparation

Solanum tuberosum peels were collected from local chips sellers around Jimma university main campus without any cost, washed several times with tap water to remove rubbish, mud followed by distilled water and shade dried at room temperature. The dried sample was ground into fine powder with mortar and pestle, and then the aqueous extract of the STP was prepared by

overnight soaking of 10 g of fine powder with 60 mL of distilled water and 40 mL of ethanol in 250 mL volumetric flask and then heating at 40 °C for 30 min. After cooling to room temperature, the extract was filtered by using Whatman No.1 filter paper thrice and the supernatant was kept in a refrigerator in order to be used for phytochemical screening and ready for CuO NPs and Ag-CuO NCs synthesis ,with slight modification [56].

3.3. Phytochemical test of *Solanum tuberosum* peel Extract

3.3.1 Test for Flavonoids

Alkaline reagent Test: 2 mL of STP were mixed with 5 mL of 1M NaOH. The presence of flavonoids was confirmed by the formation of the intense yellow color [57].

3.3.2 Test for Saponins

Frothing Test: About 2 mL of the extract was diluted separately with 20 mL of distilled water and shaken in a graduated cylinder then kept for 15 min.A 1 cm layer of foam was formed which indicates the presence of saponins [58].

3.3.3 Test for Tannins and Phenolic Compounds

Ferric Chloride Test: 2 mL STPE was treated with a few mL of 5% neutral ferric chloride. The formation of a dark blue and or bluish-black color revealed the presence of tannins and phenol [59].

3.3.4. Test for alkaloids

Wagner's Test: 2 mL of the extract was acidified with 1 mL of 1.5% v/v of HCl and 1 mL of Wagner's reagent was added. The appearance of alkaloids was indicated by the formation of yellow and/or brown precipitate [60].

3.4 Optimization of synthesis parameters studies.

Concentration of precursor salt $Cu(NO_3)_2.3H_2O$

Formation NPs was studied by varying concentrations of $Cu(NO_3)_2.3H_2O$) from 0.05 M, 0.1 M and 1.5 M and by keeping other parameters constant [61].

Volume of *Solanum tuberosum* peel extract

Three different volume of extract were taken 5 mL, 10 mL and 15 mL to synthesize CuO NPs and Ag-CuO NCs by keeping other parameters constant [62].

pH of solution

The pH in aqueous medium can have a strong influence on the process of the metal ion reduction reaction. The role of pH on NPs synthesis was seen in its effect on the capping and stabilizing potential and on NPs growth [63].Accordingly ,pH 3.5,8,9 and 10 were adjusted by adding of 1 M HCl and NaOH solution drop wisely.

Reaction temperature

The temperature recommended for the synthesis of CuO Nps and other metallic oxide NPs using plant extracts was in the range of 25–100 °C. However, higher temperature has been reported to cause poor synthesis of nanoparticles due to inactivation of biomolecules liable for the reduction of the metal salt precursor. Due to, the synthesis were studied at three different synthesis temperatures (50, 60, and 70 °C) to achieve the optimum amount of extract for the reduction of Cu^{2+} and Ag^{+} into Cu^{0} and Ag^{0} [64].

Reaction Time

The quality and type of NPs synthesized using green technology are greatly influenced by length reaction time. Accordingly, the time duration for synthesis were varied for 1 h, 2 h, and 3 h to get optimum time [65].

Amount of Ag dopant

Ag-CuO NCs absorption peak was affected by the amount of dopant. To view the effect the amount of dopant (Ag) was vary (3%, 5% and 7%) while other parameters was kept constant. In general, CuO NP and Ag-CuO NCs were synthesized using optimized parameters. In this study, an optimized approach for the synthesis of CuO NP and Ag-CuO NCs with shorter wavelength and sharp peaks was achieved.

3.5. Synthesis of copper oxide nanoparticle (CuO NPs)

Phytocapped synthesis of CuO NPs was carried out with minor modifications the following protocol described by [34]. About 50 mL solution of 0.1M Cu $(NO_3)_2.3H_2O$ was stirred for 20 min, then 10 mL of *solanum tuberosum* peel extract was added drop wisely. Then mixture was continually stirred for 30 min until homogenized well. 0.1 M NaOH was added slowly drop by

drop under vigorous stirring up to pH 9. Consequently, the solution was stirred at 60 °C for 2 h and the mixture was changed from green to dark green color, indicating the formation of CuO NPs. Then, the resulting precipitate was separated using a centrifuge at 8000 rpm for about 10 min, and filtered to remove unreacted material, and washed several times with distilled water followed by ethanol to remove impurities. The obtained, filtrate was collected on a watch glass and dried in an oven at 50 °C for 3 h. Finally, it was grinded with mortar and pestle black colored CuO NPs were obtained.

3.6 Synthesis of silver doped copper oxide nanocomposite (Ag-CuO NCs)

This synthesis methodology was adopted from previous report [66],with slight modification. To synthesize 5% Ag-doped CuO NCs, About 95 mL of solution of 0.1 M Copper (II) nitrate trihydrate was stirred for 20 min and 5 mL of 0.1M Silver nitrate solution was added drop by drop followed by the addition of 10 mL of STP extract drop wisely stirred until homogenized. 0.1 M NaOH was added drop by drop up pH 9. Then the resultant solution was stirred at 60 °C for 2 h. Subsequently, the solution was filtered with WhattmaNo.1 and washed several times with distilled water and followed with ethanol to remove the impurities. Finally, the obtained filtrates were dried at 50 ^{o}C for 3 h in an oven. Lastly, the obtained black colored of 5% Ag-CuO NCs was grinded with mortar and pestle and stored for further characterization and applications.

3.7 Characterization of CuO NPs and Ag-CuO NCs

The synthesized CuO NPs and Ag-CuO NCs were dissolved in distilled water and characterized by UV-Vis spectroscopy (jenway) between 200 and 800 nm ranges. The spectrophotometer recorded the intensity of absorbance using a quartz cuvette and distilled water was used as a reference. Generally, surface plasmon resonance of synthesized nanoparticles and energy band gap were analyzed by UV-Vis spectroscopy [32]. The FT-IR spectra were recorded in 4000-400 cm^{-1} and used to identify the presence of functional groups and to receive valuable information regarding the presence functional groups found in sample as KBr discs pest on a Perkin Elmer. It was used to obtain an infrared spectrum of absorption/emission of solid and gather spectral data in an extensive spectral range. The crystallinity and crystalline phase of synthesized samples were determined through X-ray diffraction (XRD) profiles (DR AWELL XRD -700 using 2CuKα radiation) in 2θ range of 10^{o} to 80^{o} with a scan speed of 0.03° /min [35]. The surface

morphology or structural analysis of the synthesized sample was inspected using SEM [33]. Images of the sample were taken, and a size distribution histogram of the CuO NPs and Ag-CuO NCs was made using Image J software.

3.8.Applications of CuO NPs and Ag-CuO NCs.

3.8.1 Antimicrobial activity

The antimicrobial potential of the synthesized CuO NPs and 5% Ag doped CuO NCs were screened for their invitro antimicrobial activities against bacteria strains (*S. aureus, B.Cereus S.thyphi and E. coli)*, and antifungal activities against Candida albicans by disc diffusion method at Jimma University, Microbiology laboratory.

Antibacterial activity

The bacteria strains can be first grown on agar plates at 37 ^{0}C for 24 h; prior to inoculation on to the nutrient agar. Fresh cultures of bacteria was swabbed on the surface of Mueller Hinton agar (MHA) media by using cotton swabs after solidification of the media **.**Then, the sterilized paper discs of 6 mm in diameter were dipped into the solution of concentrations CuO NPs and Ag-CuO NC (100 mg/mL) were prepared by dissolving in DMSO. Then discs impregnated with the test solutions was placed on a cultured glass plate at equidistance to one another to avoid overlap of zones of growth inhibitions and incubated for 24 h at the standard temperature for each strain, and diameters of the growth inhibition zones were recorded in mm with some modification [67]. It was going to be compared with the standard drug (Gentamicin). 10% DMSO was used as a negative control. All the above procedure was repeated three times and mean standard deviation of a zone of inhibition were taken.

Antifungal activity

The antifungal potential of the synthesized CuO NPs and Ag doped CuO NCs was studied by agar disk diffusion method, the fungal strain; *C.albinica* was spread on the MHA media using cotton swabs. Then, the sterilized paper discs of 6 mm in diameter were dipped into concentrations of CuO NPs and Ag-CuO NCs (100 mg/mL). Then discs impregnated with the test solutions was placed on a cultured glass plate at equidistance to one another to avoid overlap of zones of growth inhibitions and incubated at 37 °C for 48 h and diameters of the growth inhibition zones were recorded in mm [52]. Clotrimazole and DMSO were used as positive and

negative control respectively. All the above procedure was repeated three times and mean standard deviation of a zone of inhibition were taken.

3.9 Antioxidant activity

DPPH radical scavenging assay

The antioxidant activities of the CuO NPs and Ag-CuO NCs were performed on the basis of the free radical scavenging activity by the DPPH with some modifications in predefined method [19].0.1 mM DPPH was prepared by dissolving with methanol and the solution was coated with aluminum foil and kept in the dark until use. Then 2 mL of DPPH solution were mixed with 1 mL of different concentrations (100, 50, 25, 12.5, 6.25, 3.12 and 1.56 µg/mL) of the synthesized CuO NPs, 5% Ag-CuO NPs and Ascorbic acid used as the reference standard. 2 mL DPPH solution were used as the control. The reaction mixture was shaken vigorously and incubated at room temperature in the dark for 30 min. Then, the absorbance was recorded spectrophotometrically at 517 nm. Finally, the antioxidant activity of the synthesized CuO NPs and 5% Ag-CuO Nps were estimated based on the percentage of DPPH radical scavenged according to the following equation 2.

$$\% A_a = (A_o - A_i)/A_o \; X \; 100 \ldots\ldots\ldots\ldots\ldots\ldots\ldots\ldots (Equation2)$$

Where, Aa means antioxidant activity [%], A_i- absorbance of the sample solution, A_o means absorbance of the DPPH solution. The experiments were carried out in thrice and IC_{50} value was determined by a linear regression curve.

3.10. Photocatalytic degradation of MB dye

The photocatalytic efficacy of CuO NPs and Ag-CuO NCs was evaluated during the degradation of MB dye in the presence solar light in month April between 11 a.m to 2 p.m was studied previous method with slight modification[8]. At first, 30 mg of CuO NPs and Ag-CuO NCs were dispersed in 100 mL of MB dye solution (10 mg/L) in a beaker. Then the mixture was stirred magnetically for 1 h in a darkness to reach the adsorption-desorption equilibrium. Afterwards, the suspension was exposed to direct sunlight for 120 min. The sunlight degradation of the dye was determined by measuring the reduction in the intensity of MB at λ_{max} = 666 nm using a UV-

Vis, spectrometer at regular interval of 20 min. The degradation of dye percentage (R) was determined using equation 3:

$$\%R = [(A_0 - A_t)] / [(A_0)] \times 100 \quad \text{(Equation 3)}$$

Where A_0 is the initial absorbance of a dye and A_t is the absorbance at time t. In order to obtain the most effective degradation conditions, parameters such as the effect of the pH of MB solution, initial concentration of MB solution and photocatalyst amount were investigated.

Determination of point of zero charge of CuO NPs and Ag-CuO NCs

The point of zero charge (pzc) is the pH at which the total number of positive and negative charges on its surface becomes zero. The pH at the pzc of CuO-NPs and Ag-CuO NCs were measured by using the pH drift method. The pH of 10 mL of 0.1 M NaCl solution was adjusted between 3-12 by adding either HCl or NaOH. The 0.03 g of photocatalysts were added in 10 mL of the solution in tube and shook in shaker for 12 h then left at room temperature for 12 h. After the pH stabilized, the final pH was recorded. Then the graph of pH was drawn and used to determine the points at which the initial and final pH values were equal [68].

Reusability and stability studies

The reusability and recovery of the CuO NPs and Ag-CuO nanocatalyst towards the degradation of MB dye was studied using a method reported previously [69]. Two cycles were conducted and after each cycle, the photocatalyst was removed from the solution through centrifugation at 8000 rpm for five min, washed two times thoroughly with deionized water followed with ethanol, and then dried in an oven for 60 min at 50 °C for next cycle.

4. RESULTS AND DISSCUSION

4.1 Phytochemical analysis of the *Solanum tuberosum* peel extract

The biomolecules present in plant extracts are safe and have been employed in the treatment of diseases from pre-historic times when compared to the artificial drugs. The qualitative phytochemical test helps to reveal bioactive compounds found in *Solanum tuberosum* peel extract those can be used in the synthesis of NPs and NCs by using standard reagents shown in (figure 10).The color intensity or the precipitate formation was used as analytical responses to these tests. This result had strong agreement with chemical tests of plant extracts reported in literature [70].

Figure 10. Chemical tests of different bioactive molecules in *Solanum tuberosum* peel extract

The presence of secondary metabolites in *Solanum tuberosum* peel extract such as phenolic, alkaloids, flavonoids, tannins and saponins were tested by color confirmatory test. This confirmatory test revealed that there are bioactive constituents used to reduce Cu^{2+} and Ag^{+} into nanoscale zerovalent atom by donating of electrons and simultaneously act as effective capping agent to prevent the NPs and NCs agglomeration. Also the presence of these bioactive constituent Hydroxyl (O-H) and carboxyl (C=O) functional groups or atoms with unshared pairs of electrons used for the reduction metal ion in the precursor solution were also identified by FT-IR spectroscopy analysis.

The most important bioactive constituents found in *Solanum tuberosum* peel extract were summarized in table 1 as follows. This result is in good agreement with the previous literature reported [71].

Table 1 .Phytochemical Constituent of *Solanum tuberosum* peel extract

R/No	Phytochemical constituents	Chemical tests	Results
1.	Phenolic	Ferric chloride test	+++
2.	Alkaloids	Alkaline reagent test	++
3.	Tannins	Lead sub acetate test	+++
4.	Saponins	Frothing test	+++
5.	Flavonoids	Wagner's test	++

N.B (++) indicates the presence of phytochemicals, (+++) also indicates rich amount of phytochemicals found in the extract used as reducing, stabilizing and capping agent.

4.2 Optimization of synthesis parameters

4.2.1 Effect of concentrations of precursor salt

In present study three different concentrations of Cu $(NO_3)_2.3H_2O$ were prepared in 100 mL separate volumetric flask was done with slight modification [72]. Thereafter, 50 mL (0.05 M, 0.1M and 1.5 M) were singularly reacted with 10 mL of *Solanum tuberosum* peel extract. The mixture were homogenized vigorous stirring at 1000 rpm; green color formed indicates the formation of copper complex with different functional groups found in *Solanum tuberosum* extract and 0.1 M was optimized (appendix 1) because it gave a sharp peak which shows the formation of small sized nanoparticles since the sharpness of the surface Plasmon peak has direct proportionality with the concentrations of synthesized NPs in the solution. The result obtained was in good agreement with a recent report [73].

4.2.2 Varying Volume of *Solanum tuberosum* peel extract

After selection of optimum precursor concentration, to attain an optimum condition for the green synthesis of CuO NPs the ratio of the volume of *Solanum tuberosum* peel extract must correspond to the concentration of copper precursor used. Accordingly, three different volume of extract 5 mL, 10 mL and 15 mL were mixed with 50 mL of 0.1M Cu $(NO_3)_2.3H_2O$ solution while other parameters kept constant. When the volume of plant extract increase the reduction rate also increase this indicates the presence of different functional groups could easily donate electron to

metal precursor responsible for reduction and 10 mL was optimum volume because it gave sharp peak which indicates the reduction of Cu^{2+} into nano scaled zerovalent CuO NPs (appendix 2), on the other side the ratio of both are not corresponding to each other there was formation of broad peak with saturated amount of extract indicates large sized NPs formation in UV–Vis spectroscopy analysis results which has close agreement with literature reported previously [74].

4.2.3 Effect of pH of the solution

The pH in aqueous medium can have a strong influence on the process of the metal ion reduction reaction. The pH of the solutions ($Cu(NO_3)_2.3H_2O$ and STPE) was initially 3.5. Then to adjust the pH of the solution 0.1M NaOH solution was added drop by drop from 8-10. Accordingly; pH 9 (appendix 3) was chosen as optimum due to sharp Uv-vis peak, which indicates formation of small sized NPs. The presence of the OH^- ion in an alkaline pH environment might enhance the reducing and stabilizing capabilities of the biomolecules in the extract. In general the formation of NPs was experimentally observed in basic media are more stable and smaller in size rather than acidic media, the result have a close agreement with recent literature report [75].

4.2.4 Effect of reaction temperature

In various report the temperature recommended for the synthesis of CuO Nps and other metallic oxide NPs using plant extracts was in the range of 25–100 °C. However, higher temperature was caused poor synthesis of NPs due to inactivation of biomolecules liable for the reduction of the metal salt precursor. In our study three temperature scales (50 -70 ^oC) were adjusted with the same amount of solution followed by same step. As the temperature increased from 50 to 70 °C the absorption intensities were increased, especially at 60 °C a sharp peak was formed indicates small sized NPs formation (appendix 4), 60 °C was assumed to be the optimal temperature for the synthesis of CuO NPs.

4.2.5 Varying reaction time

The quality and type of NPs synthesized using green technology are greatly influenced by length of time for which the reaction takes place. Appendix 5 shows a small intensity peak at 1 h, and the intensity of the band increases and the peak narrows as time progressed to 2 h, beyond the optimum time (2 h), the absorption peak decreased due to the longer reaction time, revealing NPs aggregation rather than nucleation. Accordingly, optimum time required for the synthesis of CuO

NPs was 2 h, which was chosen with sharpness of peak from spectroscopic analysis which has close agreement with biosynthesis of NPs [76].

4.2.6 Effect of amount of dopant

The absorption peak of CuO NPs was affected by volume of dopant. From the UV-Vis spectra (appendix 6), various amounts (3%, 5% and 7%) of dopant (Ag) were added for optimal response. According to uv-vis spectral analysis result 5% dopant volume was chosen because it gave longest wavelength (redshift) around 352 nm where as 3% and 7% Ag-CuO NCs showed maximum absorption peak around 348 nm and 350 nm (blue shift) respectively. The amount of Ag solution could affect the absorption peak of CuO NPs to red shift; which indicates the decrease in band gap energy which was related to enhancement of overall activities of CuO NPs in antimicrobial and photocatalytic activities by production of concentrated amount of ROS.

4.3 Synthesis of CuO NPs

During the synthesis of CuO NPs the optimized synthesis parameters was chosen and mixed up in singular synthesis condition. For synthesis of CuO NPs, 50 mL of 0.1M Cu $(NO3)_2.3H_2O$ was reacted with 10 mL of *Solanum tuberosum* peel extract .The mixture were homogenized by vigorous stirring at 1000 rpm; green color formed indicates the formation of copper complex with different functional groups found in *Solanum tuberosum* extract. 0.1M NaOH were added drop by drop under stirring until at pH 9.Then the mixture was heated at 60 ^oC for 2 h green color changed into dark green indicates the formation of $Cu(OH)_2$. Then the resulting precipitate was centrifuged for 10 min at 8000 rpm and filtered to remove unreacted material; followed by washing with ethanol and double distilled water to remove impurities found in the precipitate. Lastly, it was dried at 50 ◦C in oven for 3 h and black colored CuO NPs powder (appendix 7) was obtained.

4.4 Synthesis Ag-CuO NCs

For synthesis of 5% of Ag- CuO NCs, Equimolar (0.1M) of 95 mL of Cu $(NO_3)_2.3H_2O$ and 5 mL of $AgNO_3$ solution was mixed in 500 mL beaker and then 10 mL of *Solanum tuberosum* extract was added at constant stirring at 1000 rpm until homogenized.0.1M NaOH were added drop by drop under stirring until at pH 9 and the mixture was heated at 60 ^oC for 2 h the green color changed into dark green color indicates the formation of Ag-CuO NCS. Then the dark green precipitate was centrifuged for 10 min at 8000 rpm and filtered to remove unreacted material;

followed by washing with ethanol and double distilled water to remove impurities. Lastly, it was dried at 50 ◦C in an oven for 3 h and black colored Ag-CuO NCs was obtained. The schematic presentation to synthesis of Ag-CuO NCs were clearly shown in (figure 11) below.

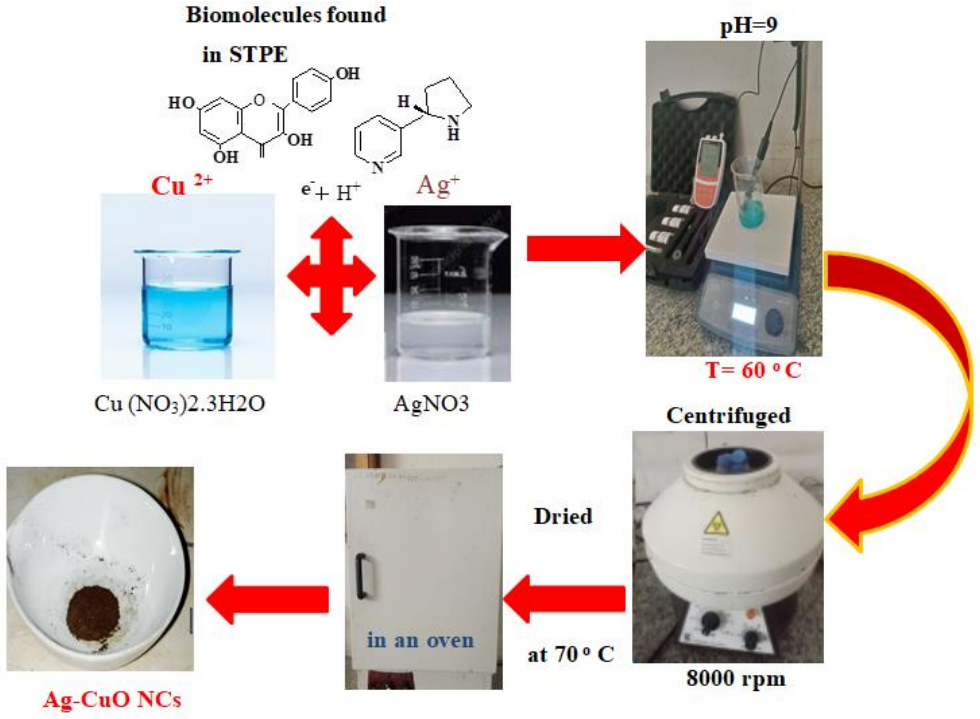

Figure 11.Schematic presentation of synthesis of Ag-CuO NCs using solanum *tuberosum* peel extract.

4.5 Characterization of synthesized CuO NPs and Ag-CuO NCs.

4.5.1 UV-Vis spectroscopy analysis

The UV-Vis spectra of the synthesized NPs and NCs were recorded in the range of 200 –800 nm at room temperature. The synthesized NPs displayed the characteristic surface Plasmon resonance (SPR) band in the spectral range of 300 nm to 352 nm. This was in line with the study conducted by literature [77],that report optimum absorbance of CuO NPs at 303 nm and Ag- CuO NCs were resulted by giving maximum absorbance at 352 nm shown in (figure 12). The peak obtained in this work is even sharper and more intense than some other works on the green synthesis of CuO NPs. This is expected to be the effect of the smaller size of the as synthesized CuO NPs. Therefore, the color changes and the UV-Vis values are taken as confirmatory results for the formation of the CuO NPs.

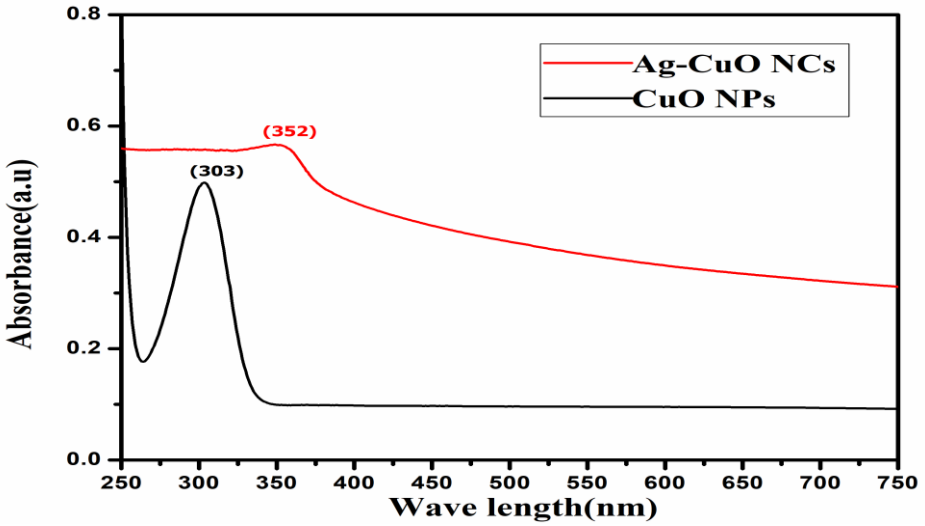

Figure 12.Uv-vis spectra of green synthesized CuO NPs and Ag-CuO NCs

From the UV-Vis spectral analysis the biosynthesized CuO NPs shows blue shift and narrow peak which indicates the formation of small sized CuO NPs with comparing to 5% Ag-CuO NCs; which shows red shift and broad peak indicates the formation of large sized NCs. The optical bandgap energy (E_g) and absorption coefficient (α) were linked by the Tauc equation with photon energy (hν) on the X-axis and a quantity $(\alpha h\nu)^{\wedge 2}$ on the Y-axis and extrapolating the linear absorption of the curve to the X-axis give the E_g of the material. The band gap energy of CuO nanoparticles was estimated to be 2.91 eV shown in (figure 13 a). This band gap energy is larger than the value reported for bulk CuO (1.9–2.1 eV).Which indicates the generation of a greater conductivity could be related to the quantum confinement effect that is the band gap increase with a reduction in particle size into nanoscale shown in (table 2) than those produced by conventional chemical techniques. This result had a close agreement with recent literature report [66] . However, this band gap is reduced to 2.67 eV after doping of silver ion shown in (figure 13 b) shows that E_g decreases as the particle size increases due to formation of Ag-CuO nanocomposites between different ionic radii of Cu^{2+} and Ag^{+} metal ion. Moreover, the decrease bandgap energy by silver doping enhances photocatalytic and antimicrobial applications by decreasing electron-hole recombination rate by improving absorbance of light in the visible range to extend lifetime of photoinduced electron-hole process.

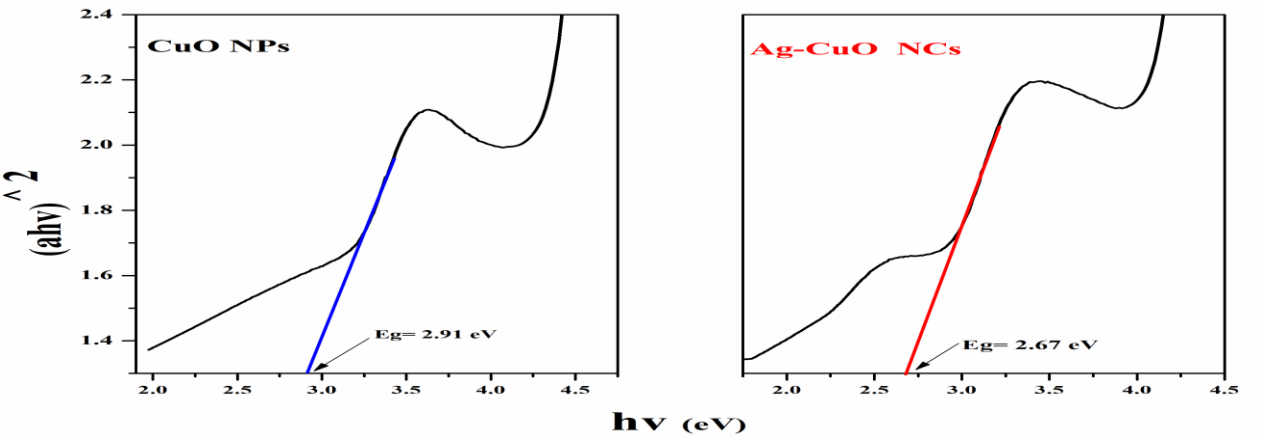

Figure 13 .(a) Tauc plot of CuO NPs and (b) Tauc plot of Ag-CuO NCs

Table 2 .Comparison b/n bandgap energy of green synthesized CuO NPs from plant extracts.

Plant extracts	Bandgap energy (eV)	Reference
Muntingia calabura Leaf extract	3.65 eV	[78]
Tinospora cordifolia Leaf extract	3.31 eV	[79]
Abelmoschus esculentus(okra) fruit extract	3.2 eV	[80]
Moringa olifera leaf extract	2.8 eV	[66]
Solanum Tuberosum Peel extract	2.91 eV	**Current study**

4.5.2 Fourier Transform Infrared (FT-IR) Spectrometry Analysis

FT-IR spectroscopy analysis was carried out to identify various functional groups responsible for reduction, stabilizing and capping agent for synthesis of CuO NPs and Ag-CuO NCs. In order to have a good understanding of the formation of CuO NPs and Ag-CuO NCs, the *Solanum tuberosum* peel extract was imparted for FT-IR to compare with that of biosynthesized CuO NPs and Ag-CuO NCs.

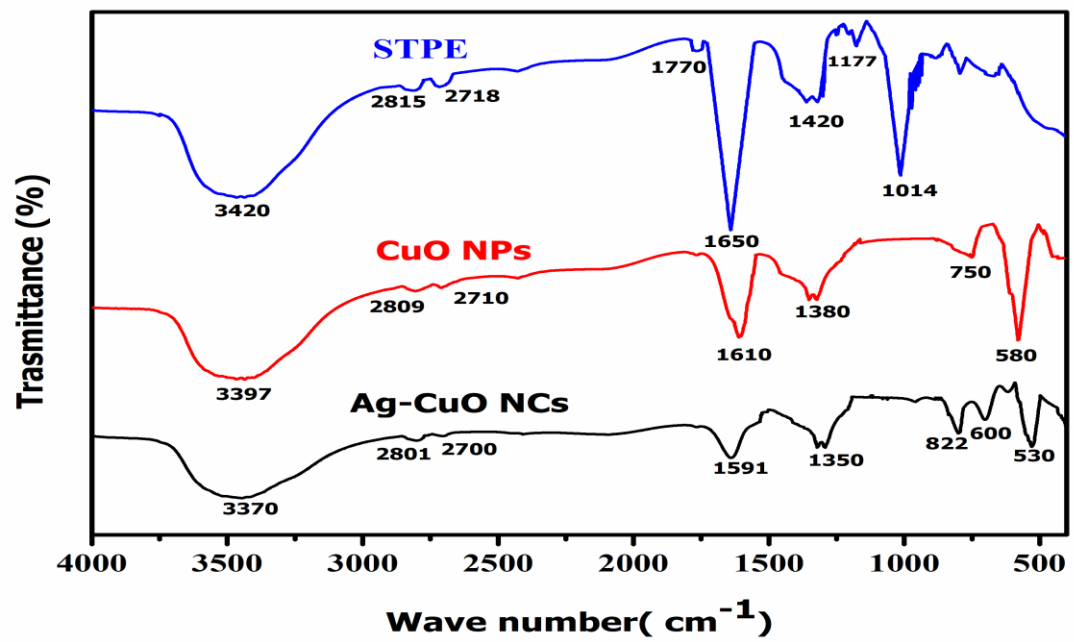

Figure 14. FT-IR spectrum of the STPE, CuO NPs and Ag-CuO NCs

From figure 14, the very strong absorption band observed in STPE around 3420 cm^{-1} corresponds to N–H/C–H/O–H stretching of amines, amides, and alcohols [81]. The peak at 2815 cm^{-1}, 2718 cm^{-1} was attributed to C–H and N–H stretching mode of secondary amines and methylene group [82]. The sharp peak around 1650 cm^{-1} shows the presence of C=O and the absorption peak at around 1420 cm^{-1} ,1177 cm^{-1} and 1014 cm^{-1} corresponds to the C–O stretching vibration of starch composition [16].The FT-IR spectrum of biosynthesized CuO NPs and Ag-CuO NCs illustrated a decrease in the peak intensities and shift of bands of the functional groups suggesting the involvement of these functional groups in the synthesis of NPs and NCs. The FT-IR spectra of biosynthesized CuO NPs and Ag-CuO NCs showed a sharp and intense absorption peak at 822 cm^{-1}, 750 cm^{-1},600 cm^{-1}, 580 cm^{-1} and 530 cm^{-1} which were not observed in STPE, expressing the stretching vibration of Cu–O and Ag–O in CuO NPs and Ag-CuO NCs respectively. Previous reports have confirmed that the absorption peaks of MOs are in the range below 1000 cm^{-1} and the obtained result is in agreement with a recent literature report [83].This agrees with the conclusion that *Solanum tuberosum* peel extract composed of polyphenols, flavonoids, alkaloids and tannins which was confirmed by qualitative phytochemical analysis and used as reducing and capping agents for the synthesis of NPs and NCs.

4.5.3 X-Ray Diffraction (XRD) Analysis

The crystallinity and crystal size of the biosynthesized CuO NPs and Ag-CuO NCs were delineated in figure 15 below shows the major peaks in the (2θ) range from 10º to 80º. The diffraction peaks at 2θ = 32.5°,35.4°, 38.6°, 48.7°, 53.2°, 58.0°, 61.3°,66.2°,68.0°, 73.4°, and 75.24° that corresponds to (-110), (002), (-202), (202), (-113), (-311), (-220), (311), (−220), (311), and (−222) planes of monoclinic CuO diffraction planes, which was well matches to the JCPDS card (no.: 45−0937) [84]. The sharp peaks with a narrow width and without any characteristic peaks of impurities were detected, suggesting that high-quality crystalline CuO NPs were synthesized.

An additional peaks were obtained in the XRD spectra of 5% Ag-CuO NCs at 38.4°,46.4°, 64.45° and 77.40° corresponds to metallic silver ion that is related to the crystal planes (111), (200), (220) and (311) showing face-centered cubic silver crystals which was well matches to JCPDS card (no. 42-0874).This result is in agreement to the recent reported literature [85].

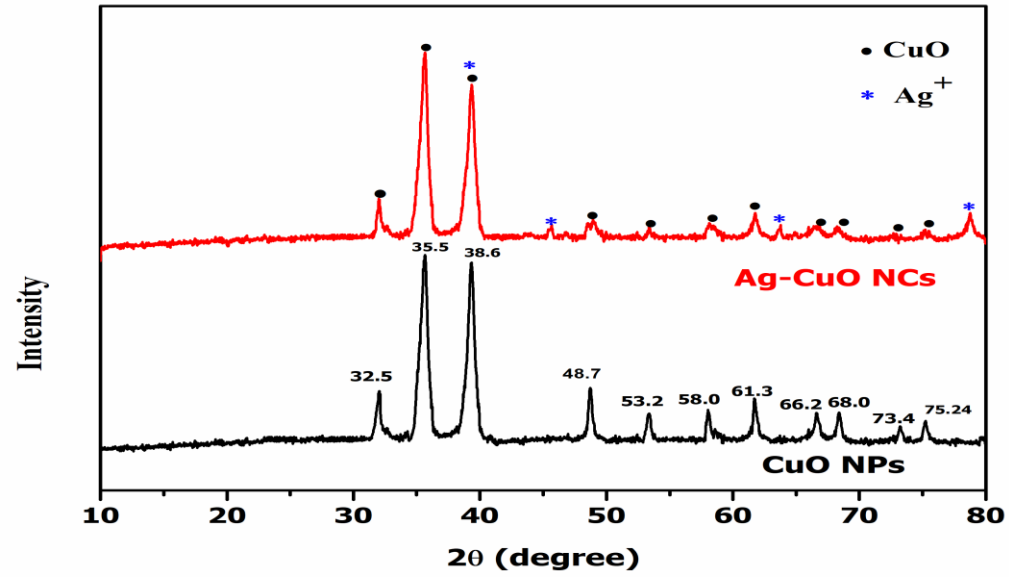

Figure 15. X-ray diffraction pattern of CuO NPs and Ag-CuO NCs

As shown in the XRD pattern, the decrease in intensity and shift towards lower angle of Ag-CuO NCs relatively is due to the effect of the doping of difference in the ionic radius between the Ag^{+} (0.144 nm) and Cu^{2+} (0.072 nm) host material, which cause the crystalline lattice to expand [86].The result is consistent with Uma *et al* [84]. As a result, Ag metal ions are at the appropriate interstitial lattice site within the crystal lattice of CuO NPs .The crystallite size

corresponding to the (hkl) plane of CuO NPs and Ag-CuO NCs were calculated using the Debye–Scherrer equation 4.

$$D = \frac{K\lambda}{\beta \cos\theta} \quad \text{(Equation 4)}$$

where D is the crystallite size (nm), k is a constant equal to (0.94), λ is the wavelength of X-ray radiation (1.5406 Å), β is the full-width at half-maximum (FWHM) of the peak expressed in radians and θ is the Bragg angle (degree) and K a constant taken to be 0.9.

Table 3.Crystalline size of synthesized CuO NPs

2 θ of Peaks	Crystal Plane	FWHM (radian)	Cos(Ɵ) (radian)	Crystallite Size (nm)	Average size (D) nm
32.5°	-110	0.009948377	0.280125345	14.50265101	**15.56**
35.4°	002	0.009075712	0.309708676	16.04065472	
38.6°	111	0.012217305	0.343306264	12.05227148	
48.7°	-202	0.009075712	0.426209403	16.77849283	
53.2°	202	0.008552113	0.465479312	18.14314712	
58.0°	-311	0.014835299	0.511468737	10.71781844	
68.3°	113	0.016755161	0.538870407	9.641626575	
73. 4°	-220	0.006283185	0.594371877	26.63543599	

Accordingly, average crystallite sizes of CuO NPs and Ag-CuO NCs were found to be 15.6 nm and 18.4 nm shown in (Table 3 and 4), respectively. However, the sizes obtained in this study were slightly smaller than those reported in the literature [87],[20] ,[66] . This may be due to the difference in the amount of reducing agents used and duration of synthesis, which can affect the size of the particles [88]. The finding correlate well with UV-Vis results discussed earlier.

Table 4.Crystalline size of synthesized Ag-CuO NCs

2 θ of Peaks	Crystal plane	FWHM (radian)	Cos(Ɵ) (radian)	Crystallite Size (nm)	Average size (D) nm
32.5°	-110	0.00837758	0.280125345	17.22189807	**18.42**
35.4°	002	0.006457718	0.309708676	22.54362285	
38.6°	111	0.010995574	0.343306264	13.39141276	
46.3° **(new peak)**	200	0.008901179	0.398109602	16.89858241	
48.84	-202	0.008028515	0.426209403	18.96699189	
58.34	-311	0.007679449	0.465479312	20.20486839	
64.45° (new peak)	220	0.015358897	0.511468737	10.35243826	
68. 3°	113	0.013788101	0.538870407	11.71640698	
73. 4°	-220	0.008726646	0.555451034	18.69986563	
77.40° (new peak)	311	0.004886922	0.594371877	34.24556056	

4.5.4. Scanning Electron Microscopy (SEM) analysis

The surface morphological features of synthesized pure and doped CuO samples were investigated by Scanning Electron Microscopy. The observed images were taken at magnifications at 3000x and 5000x (appendix8) are shown in figure 17(A and B) of the synthesized CuO NPs and Ag-CuO NCs, respectively. The result revealed that the CuO NPs had spherical particle morphology with some extent of agglomeration .This result is closely related to recent finding in the literature that reported CuO NPs [89].

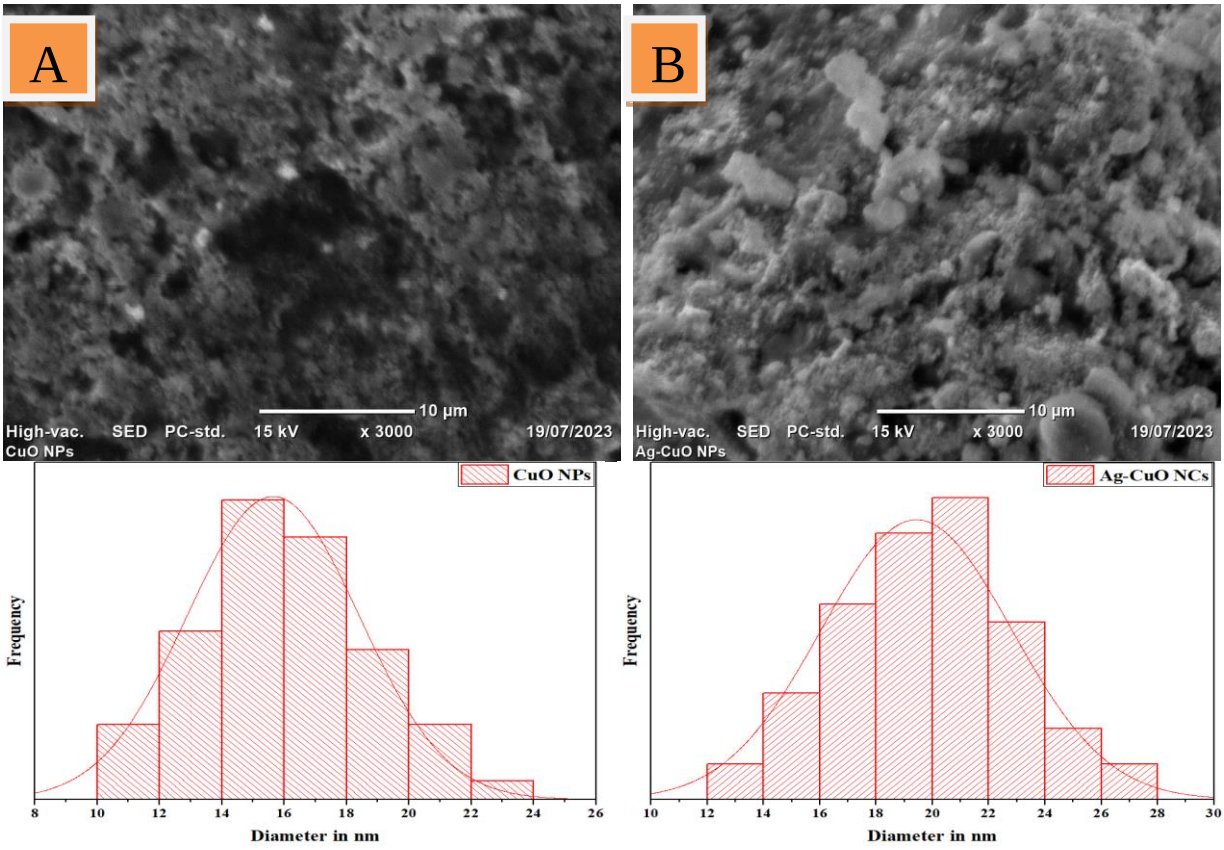

Figure 16.A and B shows SEM images and histogram of particle distribution of CuO NPs and Ag-CuO NCs respectively

In the case of Ag-CuO NCs (figure 16 B), a mixture of spherical and rod structures with a wider size distribution than CuO NPs was observed. The prepared NCs appeared a little agglomerated due to high surface area caused from small size of interparticle contact. Similar effect were seen in literature [89] . The particle distribution of NPs and NCs were ranging from 10 to 30 nm shown in (figure 16 A and B) measured by using Image J software. The obtained results are consistent with UV-Vis spectra and XRD results, which showed the formation of larger particle sizes in Ag-CuO NCs, and in agreement with previous literature reports [20].

4.6 Application of biosynthesized CuO NPs and Ag-CuO NCs

4.6.1 Antimicrobial activity of CuO NPs and Ag-CuO NCs

In our study, the antimicrobial activities of CuO NPs and Ag-CuO NCs synthesized from *Solanum tuberosum* peel extract were evaluated against with two gram-negative, two gram-positive bacteria and a fungal culture such as; *Staphylococcus Aureus* (+), *Bacillus cereus* (+), *Salmonella typhi* (-), *Escherichia Coli* (-) and *Candida Albicans* using disc diffusion. Clear zone of inhibitions were observed after 24 h and 48 h shown in (figure 17) incubated cultures supplemented with CuO-NPs and Ag-CuO NCs with concentration of 100 mg/mL were loaded discs with bacterial and fungal strain shown in (figure 17) respectively. The measurement was made in millimeter using mm scale ruler were estimated in Table 5.

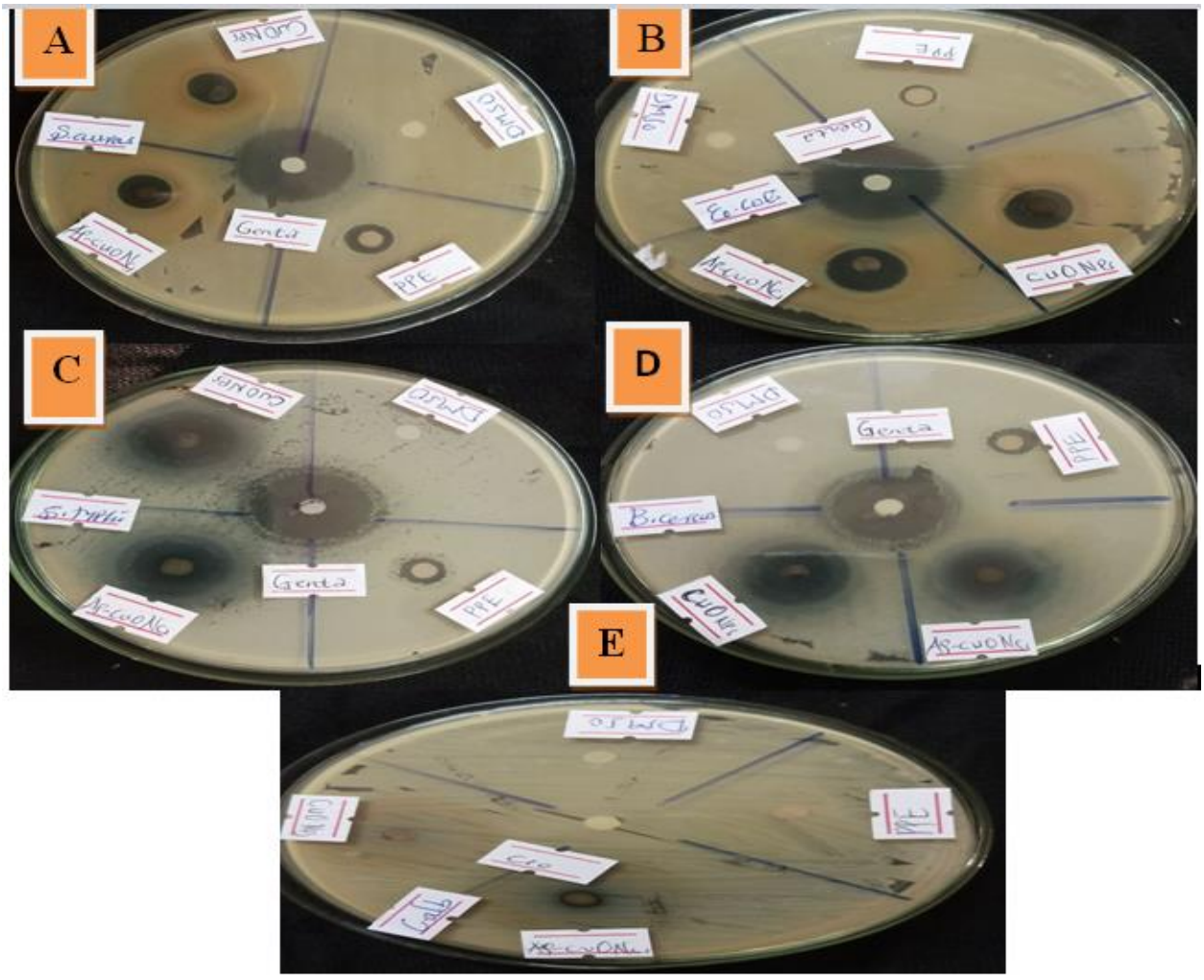

Figure 17 .Shows the zone of inhibition A), *S.aureus* B), *E.coli* C), *S.thyphi* D), *B.cereus* and E) *C.albinica* due to the effect of CuO NPs and Ag-CuO NCs in 100 mg/mL.

Table 5. Assessments of CuO NPs and Ag-CuO NCs activities against different bacterial and fungal strains at 100 mg/mL

Concentration	Mean value of Inhibition of bacterial and fungal strain									
	NPs and NCs									
	E. Coli		*S. typhi*		*S. Aureus*		*B.Cereus*		*C.albinica*	
mg/mL	CuO NPs	Ag-CuO NCs	CuO NPs	Ag-CuO NCs	CuO NPs	Ag-CuO NCs	CuO NPs	Ag-CuO NCs	CuO NPs	Ag-CuO NCs
100 mg/mL	20 ± 0.54	25± 0.54	21± 0.52	24± 0.52	21± 0.51	26± 0.50	20± 0.52	25± 0.52	16± 0.54	20± 0.56
STPE	13± 0.52		15± 0.55		16± 0.54		14± 0.52		11± 0.53	
Genta/Clo	27		28		29		29		NI	
DMSO	NI		NI		NI		NI		NI	

NB: NI- no inhibition zone were seen.

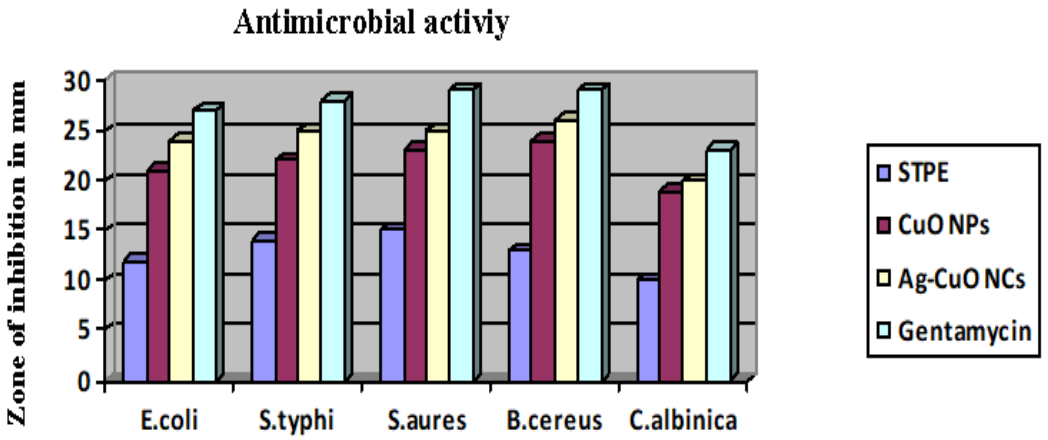

Figure 18.Comparative assessment of STPE, CuO NPs and Ag-CuO NCs on selected pathogenic strain at 100 mg/mL of concentration

The biosynthesized CuO NPs and Ag-CuO NCs show good enough antimicrobial activities towards bacterial and fungal strain. However, Ag-CuO NCs shows excellent antimicrobial activities that were comparable to that of standard drug (Genta/Clo) in both bacterial and fungal strain with maximum ZI in *S.aureus (*26± 0.50 mm), *E.coli (*25± 0.54 mm) and *C.albinica (*20± 0.56 mm). Meghana *et al*. [35], release of both Ag^{+} and Cu^{2+} metal ions easily adhered by action of

electrostatic force of attraction on the surface of fungal and bacterial cell wall causes death. The death of bacteria cell through multiple mechanisms; firstly direct interaction of released Cu^{2+} and Ag^{+} ions from NPs and NCs can easily adhere to the cell wall and cytoplasmic membrane as they are more closely related to sulfur proteins and also due to electrostatic attraction and inactivate bacteria more efficiently. At the same time, the bacterial envelope is disrupted because when Cu^{2+} and Ag^{+} ions attach to the cell wall or cytoplasmic membrane, it enhances the permeability of the cell and ultimately leads to cell disruption. Secondly; when free Cu^{2+} and Ag^{+} ions are uptaken by cells, they deactivate respiratory enzymes, generating ROS interrupting ATP production[90]. The oxidative stress induced by excess of ROS can destroy intracellular bio-macromolecules, such as proteins, lipids, RNA and DNA. In DNA, the Cu^{2+} and Ag^{+} ions interact with sulfur and phosphate components and can cause difficulties in DNA replication and cell reproduction [91] shown in (figure 19).

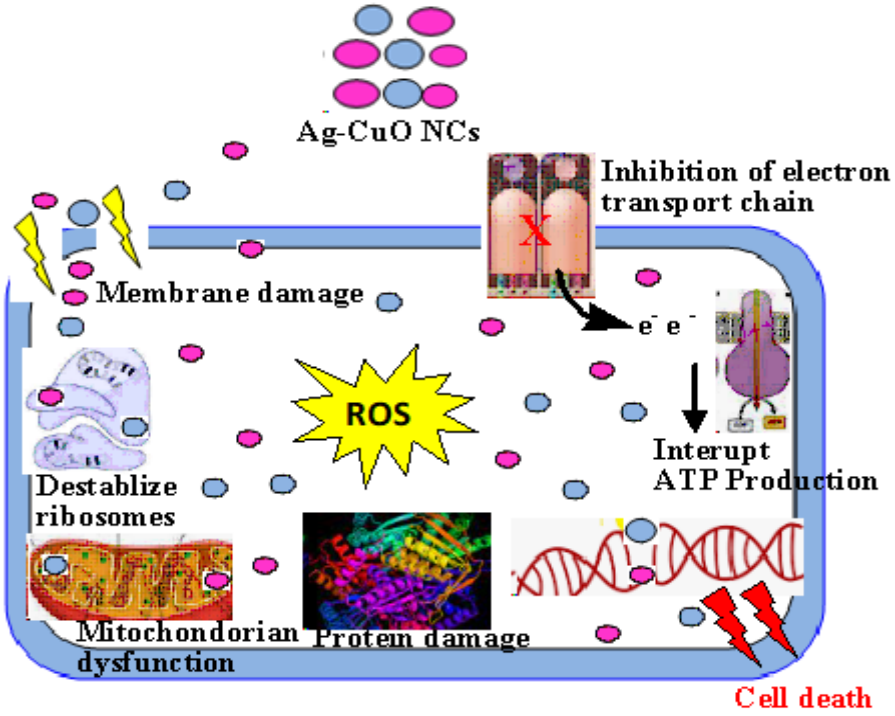

Figure 19.Antimicrobial mechanisms of Ag-CuO NCs in micro-organisms.

Here, the results showed good antibacterial activities of biosynthesized CuO NPs and Ag- CuO NCs towards gram-positive bacteria than gram-negative could be related with their cell wall structure. Gram- positive bacteria have single and thick layer of peptidoglycan in their cell walls, whereas gram-negative bacteria have a thin peptidoglycan layer with an additional outer membrane layer consisting of lipopolysaccharide causing them to be resistance.

Downright biosynthesized Ag-CuO NCs have eminent antimicrobial activity against bacterial strain than fungi, this may be due to significant difference in their cell composition meanwhile bacteria are single celled unicellular prokaryotic organisms whereas fungi are multicellular eukaryotic organisms. As a result NPs easily penetrate bacterial cell wall rather than fugal cell wall. In our investigation there was no zone of inhibition observed by standard drug (clomatrazole) in *C.albinica* species which indicates the species was drug resistance species but moderate ZI were observed in 100 mg/mL of CuO NPs and Ag-CuO NCs. Moreover, the species is more complicated organisms than bacteria. Therefore, structure complexity of the fungal cell wall results lesser diameter of zone of inhibition was observed as compared to that in bacteria similar fashion was observed in a previous report [92].

In general, it was acknowledged that Ag and Cu metal have extraordinary antimicrobial activities against wide range of micro-organism. Hence, the incorporation of Ag^{+} ions with CuO NPs had shown better inhibition zone on microbial growth due to its decreased band gap energy creates concentrated amount of ROS can destroy intracellular bio-macromolecules caused death in both Gram positive and Gram negative bacterial as well as compared to undoped CuO NPs.

4.4.2 Antioxidant activities of CuO NPs and Ag-CuO NCs

For DPPH free radical scavenging activity study the biosynthesized CuO NPs and Ag-CuO NCs concentration range from 1.56 μg/mL –100 μg/mL (appendix 9). Besides examining the results, ascorbic acid was utilized as standard. The absorbance of the reaction mixture (sample with an aliquot of 0.1 mM DPPH solution) was recorded at 517 nm [93].

In this study, the percentage of scavenging activities were determined to evaluate the antioxidant activity of synthesized NPs and NCs, which were able to inhibit free radicals . A weak inhibitory activity was found in STPE (2% - 59%). The best percentage scavenging activity was shown by Ag-CuO NCs (9%–80 %), followed by CuO NPs in all concentrations studied. The scavenging activities of Ag–CuO NCs at high concentrations (100 μg/mL) were comparable to those of standard ascorbic acid shown below in Figure 20.

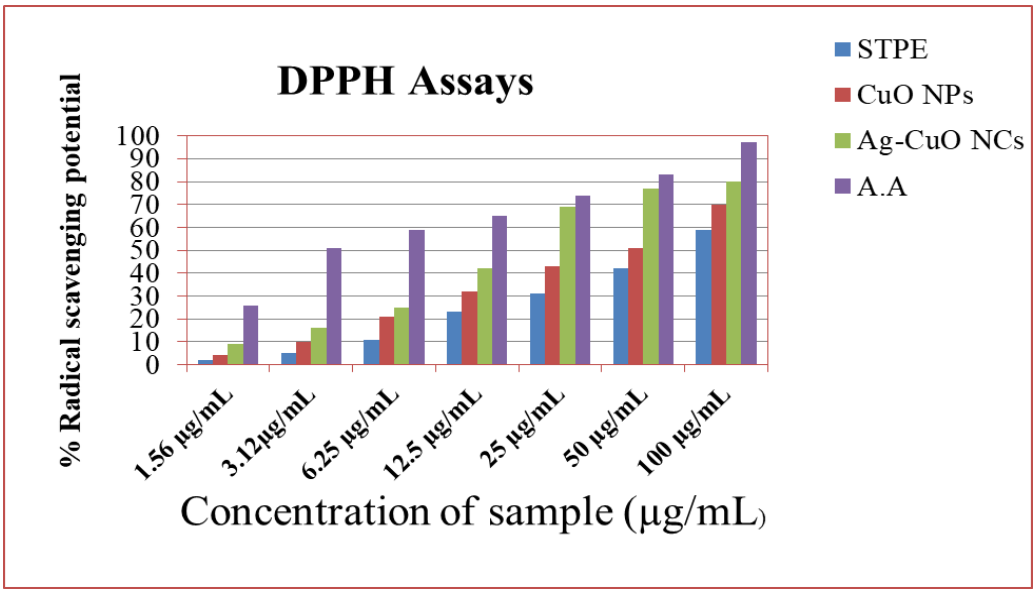

Figure 20.Antioxidant activities of the STPE, CuO NPs, Ag-CuO NCs, and AA.

Ordinarily, the efficiency of antioxidant action was revealed via IC_{50} value. IC_{50} value defined the available quantity of samples for 50 % activity. IC_{50} values were determined by the inhibition rate (%) versus the available quantity of sample through a linear regression method. The quantity of sample concentration of 50 % inhibition was calculated from the percent inhibition versus concentration plot using equation (5), to calculate IC_{50} value of sample.

$$IC_{50} = \frac{(50 - b)}{m} \quad \text{……..……. (Equation 5)}$$

Where, b indicates y – intercept value from graph and m indicates slopes from linear equation. Accordingly, Ascorbic acid displays lower IC_{50} value than Ag-CuO NCs, CuO NPs and STPE the greater its ability to neutralize free radicals. The DPPH free radical scavenging assay showed an effective distribution pattern was Ascorbic acid > Ag-CuO NCs >> CuO NPs > STPE, with calculated IC_{50} values of 4.37, 35.43, 51.55, and 65.15 µg/mL respectively. In this study, synthesized Ag-CuO NCs using STPE have shown good antioxidant activity due to capped phenolic compounds present in STP extract. The DPPH free radical scavenging activity (IC_{50} µg/mL) of SPTE, CuO NPs, Ag-CuO NCs and standard A.A, produced by different concentrations was presented in (figure 21) below.

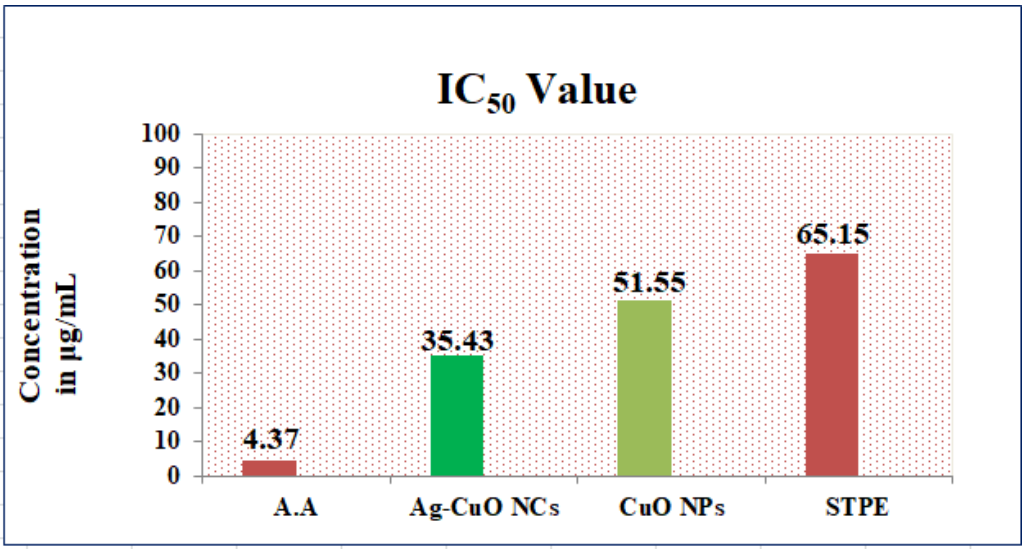

Figure 21 .IC_{50} values of A.A, Ag-CuO NCs, CuO NPs and STPE

This study reveals that STPE mediated Ag-CuO NCs are more effective at scavenging free radicals and can be used as a major antioxidant source in antioxidant-based therapies. The Ag-CuO NCs' scavenging behavior increases as the concentrations increase and the lower the IC_{50} value indicates the greater is the hydrogen donating potential of the free radical scavengers and thus their antioxidant activity.

Table 6. Comparison of antibacterial and antioxidant activities of Ag-CuO NCs synthesized by different plant species with the present study

Plant Source	**Different Bacterial Strains**	**Zone of inhibition in mm**	**Antioxidant Activity**	**IC_{50} Value**	**References**
Solanum Tuberosum peel extract	*E.coli* *S.aureus* *S.thyphi* *B.cereus* *C.albinica*	25± 0.54 26± 0.52 24±0.52 25±0.52 20±0.56	80 %	**35.43 µg/mL**	**Current study**
Malus Domestica leaf extract	*E. coli* *S. aureus*	17 19	80 %	52.78 µg/mL	[19]
Jatropha curcas leaf extract	*C.albinica*	18	70%	41 µg/mL	[94]
Fusarium nygamai isolate AJTYC1	*E.coli* *S.aureus* *C.albinica*	30 22 20	66.91%	146.58 µg/mL	[95]

4.6.3. Photocatalytic Degradation of MB dye under sunlight.

The photocatalytic activity of the biosynthesized CuO NPs and Ag-CuO NCs was investigated for the degradation of aqueous solutions of methylene blue under sunlight irradiation. The UV-VIS spectrophotometer was noted from 400 to 800 nm and the absorption peak was observed at a wavelength of 666 nm of MB dye, which is detected by the change in color of the solution from blue to colorless due to electron transfer. Factors affecting degradation of MB dye were also investigated as follows:

4.6.3.1. Effect of initial dye concentrations

The effects of dye concentration on percentage degradation were studied under sunlight irradiation by varying the initial concentrations of MB from 5 to 20 mg/L with as synthesized 30 mg NPs and NCs catalyst loading. The MB solution containing NPs and NCs was kept in dark for 1 h to achieve the adsorption-desorption equilibrium.

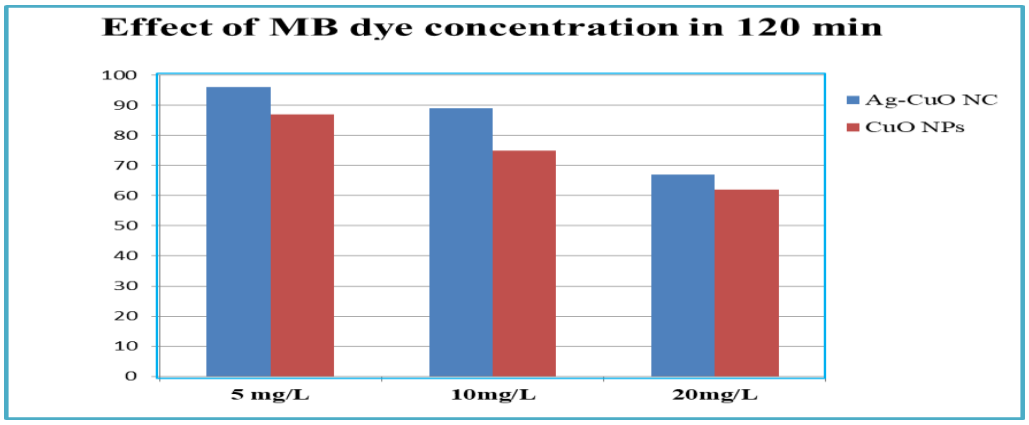

Figure 22.Effect of initial MB dye concentration on photocatalytic degradation

Above figure 22 showed that the percentage degradation of dye decreased from 96% to 73% and 87 % to 66% by NCs and NPs with increasing the initial concentrations of MB from 5 to 20 mg/L after 120 min of irradiation. These results illustrate that at lower concentrations, MB molecules are adsorbed to a large degree due to the availability of more active sites on the surface of NPs and NCs hence, the degradation efficiency is higher. In contrast, as the initial concentration of MB is raised, the MB molecules adsorbed light and the photons never reached on surface of catalyst reduce light penetration. Due to this lesser numbers of ROS are produced hence, the photodegradation of MB using biosynthesized NCs and Nps decreased; the result had

a close agreement with literature report [96]. Thus, the removal efficiency of MB dye was found to be better at low dye concentrations. It clearly shows the degradation proficiency of the catalyst is inversely related to the initial dye concentration of MB dye.

4.6.3.2. Effect of the pH of the solution

To investigate the influence of pH on MB sorption, PZC of catalyst varied from 3 to 12 by using 0.1 M NaOH and HCl.

Investigation of point of zero of charge (pHpzc) of CuO NPs and Ag-CuO NCs

For the investigation of point of zero of charge CuO-NPs and Ag-CuO NCs, 10 mL of 0.1M NaCl solution adjusted from pH 3-12 using 0.1 M HCl and NaOH, then after 0.03 g of NPs and NCs were added on it and the solution were shook the speed at 150 rpm on orbital shaker for 12 h. Next the solutions were left for 12 h at room temperature and filtered out then the pH values of the filtrate were recorded.

Table 7 . Point of zero charge of CuO NPs and Ag-CuO NCs

pH of initial solution	pH of solution after 24 h(CuO NPs)	ΔpH of the solution	pH of solution after 24 h (Ag-CuO NCs)	Δ pH of the solution
3	5	2	5.71	2.71
4	6.72		6.22	2.22
5	7.24	2.24	7.12	2.12
6	7.26	1.26	7.52	1.52
7	7.42	0.42	7.61	0.61
8	9.59	-1.39	9.22	-1.18
9	7.61	-1.59	10.51	-1.51
10	7.82	-2.18	8.42	-1.58
11	7.32	-3.68	7.89	-3.11
12	7.91	-4.09	7.65	-4.35

From the graph (appendix 10), the values of pzc of NPs and NCs were determined from the points where the initial pH equals the final pH. According to investigation pzc values for biosynthesized CuO NPs and Ag-CuO NCs are estimated to be 7.22 and 7.34, respectively.

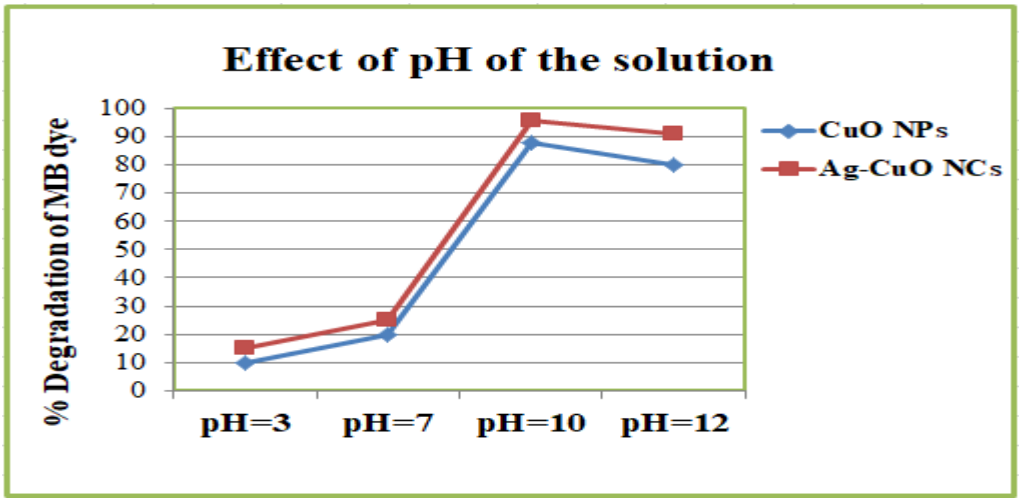

Figure 23.Effect of pH on MB degradation with photonanocatalyst.

The variation of pH alters the surface nature of NPs and NCs. Below pH_{pzc} the surface of a catalyst becomes positively charged and the MB is a cationic dye which displayed repulsive behavior hence, degradation proficiency decreases. When pH above pHPZC the catalyst surface has a negative charged more and more deprotonated, providing more and more sorption sites for MB with increased sorption efficiency which attracts the MB dye molecules to a greater extent. At pH 10 per hydroxyl, radicals are formed, leading to the formation of hydrogen peroxide which offers rise to hydroxyl radicals on a large scale. The increasing of the $^{\cdot}OH$ radicals on surface of nanocatalyst intensify active sites for degradation of MB dye. Sharma *et al.*[97] reported that hydroxyl radicals were the most important reactive oxygen species that caused degradation when CuO NPs were used. Various studies also reported a degradation of more than 95% for MB at basic conditions [98],[99],[100]. Contrarily at pH 3, the lowest degradation of 18% was noted shown in (figure 23). This is because at acidic conditions more positively charged ions are formed and when they interact with a cationic dye they tend to form repulsion, thus exhibiting minimal dye degradation. At neutral conditions though, not much degradation was noted, with only 20% to 25% of MB degraded and highest degradation was recorded at pH 10 (basic conditions) for both biosynthesized CuO NPs and Ag-CuO NCs of 84% and 97% after 120 min respectively; had a close agreement with previous literature [101].

4.6.3.3. Effect of Photocatalyst dose

The amount of catalyst used in the photocatalytic reaction may enhance the efficacy of degradation of MB dye as a result of the good dispersion of the catalyst in the aqueous medium which leads to an increase or decrease in the absorption of photons through the surface area exposed to light [72].The percentage degradation of MB was studied under different concentrations of catalysts amount in the range of 10 to 50 mg at a constant dye concentration of 10 mg/L shown below in figure 24.

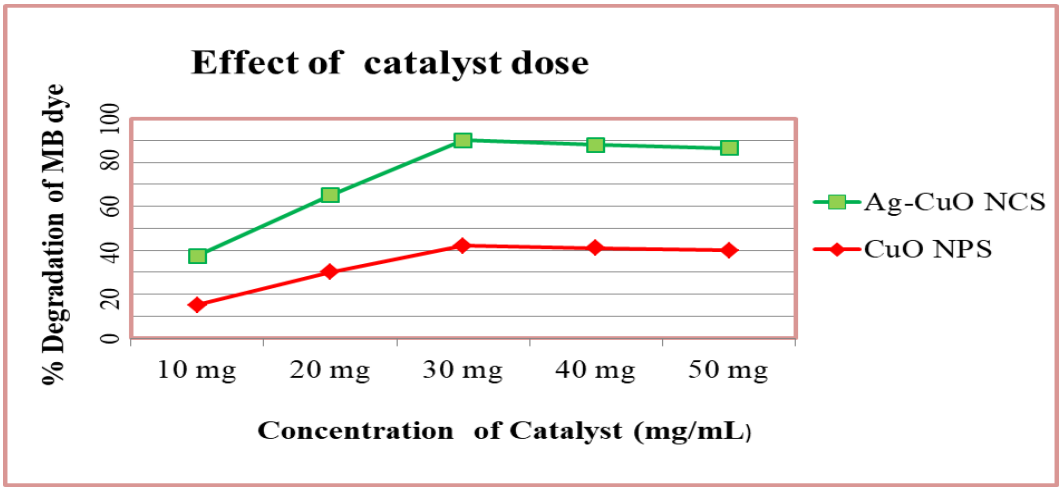

Figure 24.Effect of catalyst dose on degradation of 10 mg/mL MB dye in sunlight.

The photocatalytic activity goes linearly increasing with catalytic load up to limit 30 mg due to the uniform dispersion of catalyst and the availability of a more active site on the surface of the catalyst [99]. Accordingly, the degradation of the MB dye was improved from 30 % to 80 % and 45 % to 94% using CuO NPs and Ag-CuO NPs respectively after 120 min. It was obvious that a catalyst dose of 30 mg was optimal for photocatalytic degradation of 10 mg/L of MB dye within 120 min. But beyond the optimum amount of catalyst loading, the percentage degradation reduced due to increase in the opacity of the suspension, and thus decreasing the light scattering caused by turbidity of solution as a result less photocatalysts could be activated. Similar result were observed in previous report [102].

4.6.3.4. Effect of irradiation time

The time of exposure to sunlight was prominent factor for production of OH radical for degradation for MB dye under sunlight. The optimized 10 mg/L of aqueous solution of MB dye and 30 mg both biosynthesized CuO NPs and Ag-CuO NCs were kept in dark for 1 h to achieve

the adsorption-desorption equilibrium. The samples were analyzed by UV-Vis spectroscopy, the decrease of MB dye absorbance spectra were observed from 20 min to 120 min when compared to that of controls (Figure 25).

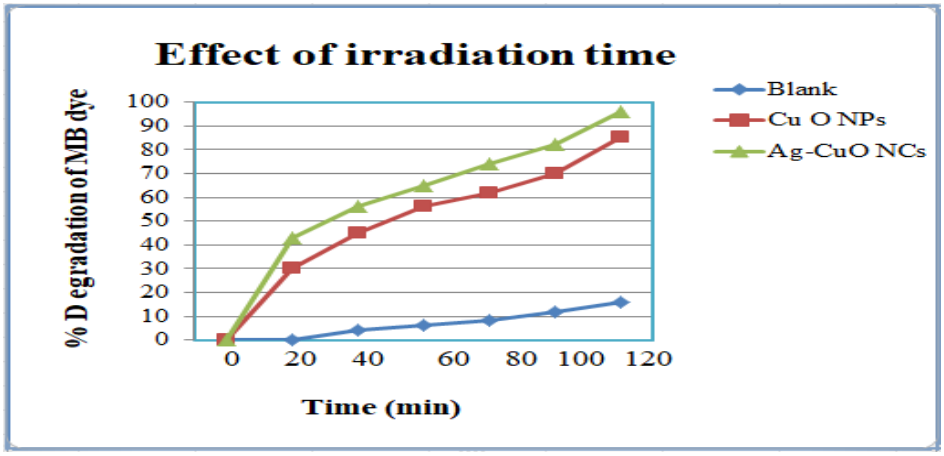

Figure 25.Effect of irradiation time on degradation of MB dye.

The result revealed that the degradation of MB and irradiation time had shown linear relation meanwhile percentage degradation increases with increasing of irradiation time from 20 min to 120 min from 30 % to 85% and 43% to 96% for both CuO Nps and Ag-CuO NCs respectively. Unlike for blank (solution stirred without sunlight) 4 % to 16 % degradation takes place due to adsorption on the surface of nanocatalyst due to their high surface area and their smaller in size.

4.6.3.5. Comparison of catalytic performance of CuO NPs and Ag-CuO NCs

For comparison, the pure CuO NPs and 5% Ag doped CuO NCs were studied under the same reaction conditions. For this purpose, experiments were performed by taking an optimized amount a 100 mL aliquot of 10 mg/L MB at pH 10 with 30 mg of the CuO NPs and Ag-CuO NCs under 120 min of sunlight light irradiation. Thereafter, the solution exposed to direct sunlight and after 20 min intervals 5 mL of supernatant were subjected by using syringe and centrifuged for 3 min at 8000 rpm, the absorbance were receded at regularly interval up to 120 min.

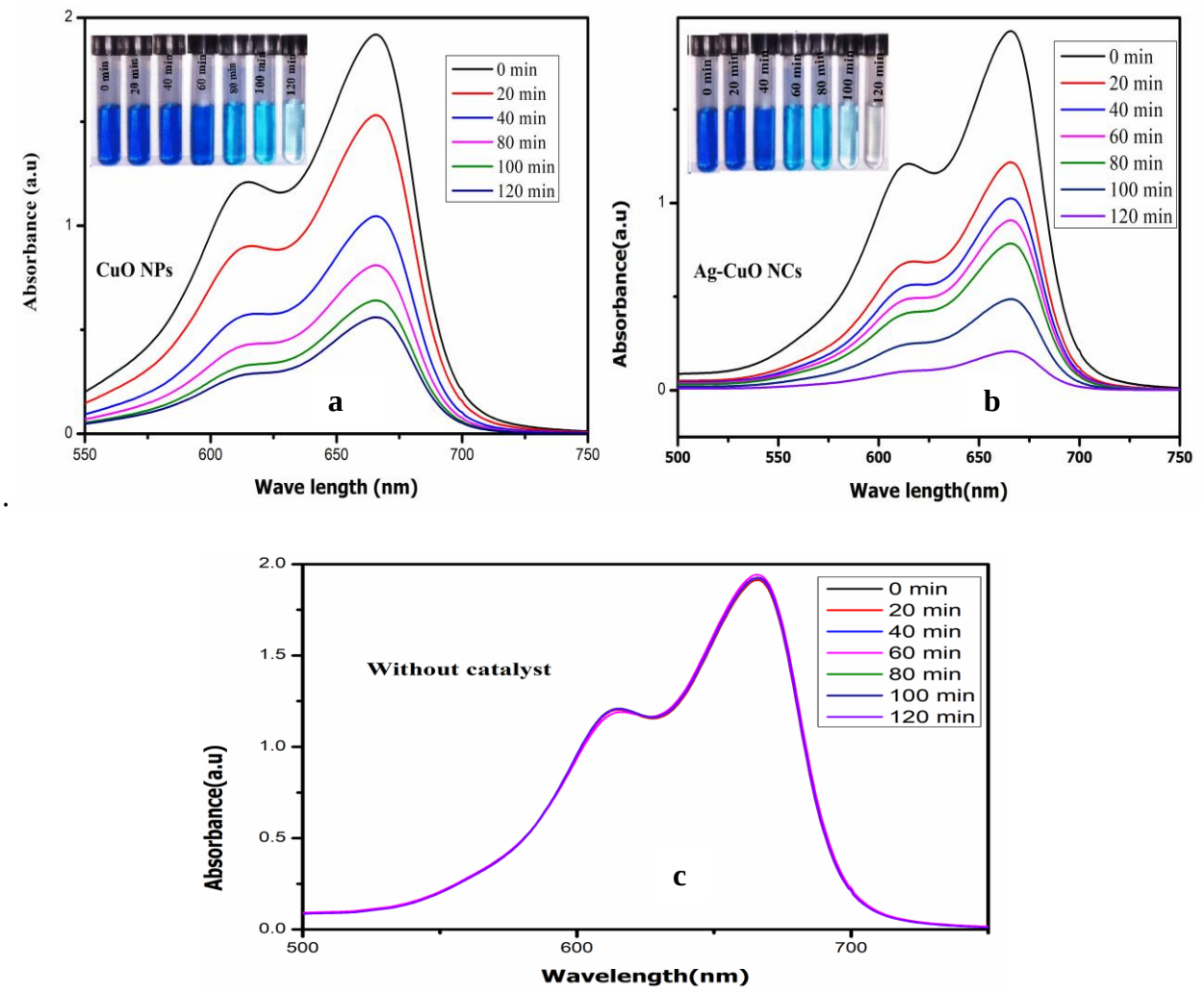

Figure 26.(a) Shows photocatalytic degradation of MB dye with CuO Nanocatalyst. (b) Shows photocatalytic degradation of MB dye with Ag-CuO NCs, and (c) shows photocatalytic degradation of MB dye without catalysts after 120 min sun light irradiation

Figure 26, clearly shows the percentage degradation of MB dye without any catalyst, no degradation of the MB dye solution occurs irradiation up to 120 min. However, the intensity of the absorbance decreases or the degradation of the MB dye increases with the increase of irradiation time in presence of catalysts. As compared to pure CuO catalyst, 5% Ag doped CuO catalysts showing better degradation efficiency with 96% and 80% respectively after 120 min irradiation time exposed to sun light. This maximum degradation efficiency may be attributed to Ag^{+} ion, which can serve as electron trapping sites, promote charge separation by inhibiting the recombination of photogenerated charge carriers. On the other hand, the confined bandgap due to Ag^{+} ion doping onto CuO NPs significantly influenced the degradation activity. The Figure (26)

shows the degradation of the dye with catalyst and without catalyst under visible light irradiation for 120 min. The result revealed that there was no degradation takes place without catalyst under sunlight irradiation after 120 min. It was undeniable that the efficiency of photocatalytic degradation is highly dependent on photocatalyst material and light source as a result, there was no degradation took place without catalyst after 120 min irradiation shown in figure 26(c).

4.6.3.6. Photocatalytic reaction mechanism

The proposed mechanism of photocatalysis (Figure 27) that Ag-CuO NCs absorbs photon at greater or equal to energy bandgap, electrons and holes are created by illumination of sunlight. Electrons in the CB of Ag-CuO NCs by photosensitization which can react with the adsorbed O_2 to produce superoxide radical anion ($\cdot O_2^-$) and on the other side, positive hole in the valence band can also abstract electron from water molecules to produce highly reactive hydroxyl radicals through oxidative process. Then $\cdot O_2^-$ and $OH^{\cdot}$ radicals can attack the functional group of the MB dye and finally oxidized into CO_2 and H_2O via radical chain mechanism [14]. Hence, the complete degradation of MB ends up producing H_2O, CO_2, and other less toxic substances as shown in (equation:6)

$$CuO + h\upsilon \rightarrow e^- (CB) + h^+ (VB)$$
$$e^- + O_2 \rightarrow \cdot O_2^-$$
$$Ag^+ + e^- (CB) \rightarrow Ag$$
$$h^+ + OH^- \rightarrow \cdot OH \ldots\ldots\ldots \textit{(Equ 6)}$$
$$\cdot O_2^- + MB \rightarrow CO_2 + H_2O$$
$$\cdot OH + MB \rightarrow CO_2 + H_2O$$

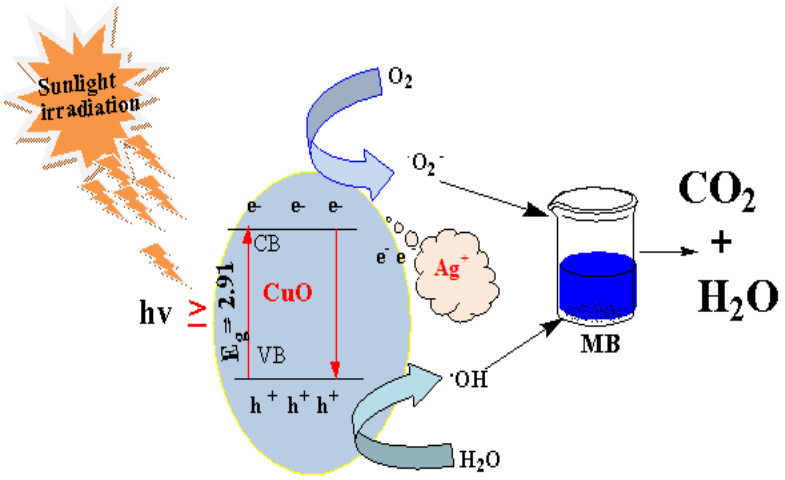

Figure 27 .Mechanisms of photocatalytic degradation of MB dyes by Ag-CuO NCs

Accordingly, 5% Ag-CuO NCs showed better percentage degradation up to 97% comparing to undoped pure CuO NPs, due to Ag ion doping to CuO NPs host material have enhanced catalytic activity by reducing e^- and h^+ recombination rate by trapping photoinduced electron and shifting the band gap towards visible region of spectrum for better absorption related for production concentrated amount of ROS for degradation.

.

Table 8.Comparison of photocatalytic degradation of Ag-CuO NCs synthesized by green method with the present study

Green source	Dye	% degradation	Time(min)	Ref.
***Solanum tuberosum* peel extract**	MB	97%	120 min	**Current study**
***Laurencia dendroidea* extract**	MB	65%	60 min	[103]
***Sida rhombifolia* leaf extract**	MB	86%	40 min	[101]

4.6.3.7. Reusability and stability performance of CuO NPs and Ag-CuO NCs

The stability of the fabricated CuO NPs and Ag-CuO NCs were investigated by recycling in repeated degradation experiments under sunlight illumination. In this studies the optimal parameters were chosen with dye concentration of 10 mg/L, pH = 10, and catalyst dose of 30 mg were taken. Before being dried in an oven at 70 °C for 2 h, the produced nanocatalysts were centrifuged at 8000 rpm for 5 min and washed with distilled water twice, and followed by ethanol after each cycle was completed and then employed in the subsequent reaction .Figure 28, shows that the removal of the MB by the CuO NPs and Ag-CuO NCs photocatalysts after the 1st cycle achieved up to 80% and 90% respectively. After the 2nd cycle, the removal of the MB decreases down to 74% and 85%.The minimally decreases, due to the unavoidable loss of photocatalysts during the cycle processes. Figure 28 shows that CuO NPs and Ag-CuO NCs have excellent stability and do not suffer from photo-corrosion during degradation, this is in line with reported literature [104].

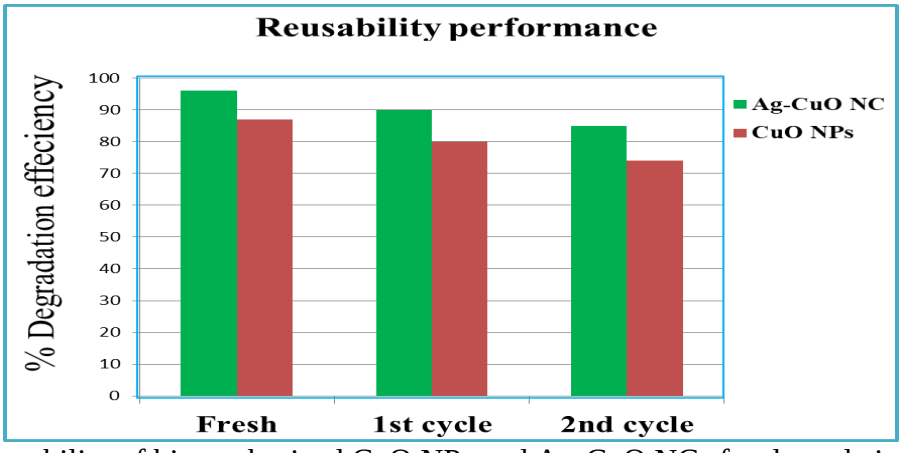

Figure 28.Reusability of biosynthesized CuO NPs and Ag-CuO NCs for degradation of MB dye.

5.CONCLUSION AND RECOMMENDATION

5.1. Conclusion

A facile, ecofriendly and economical feasible green approach were used to synthesize CuO NPs and Ag-CuO NCs using phytochemical rich *solanum tuberosum* peel extract. The synthesis of NPs and NCs using STPE as reducing agent were confirmed primarily by color change followed by Uv-visible absorption peak at λ_{max} at 303 nm and 352 nm respectively. The FT-IR result revealed the biofabrication of the NPs and NCs by the action of different bioactive molecules with their different functional groups present in the peel extract and the presence of Metal – oxygen bonds below 1000 cm^{-1}. The XRD patterns confirmed purity and crystallinity of the synthesized NPs and NCs, and the crystalline sizes of the particles formed are 15 nm and 18 nm respectively. The SEM data demonstrate that crystalline CuO NPs has a spherical and Ag-CuO NCs have a mixture of spherical and rod shapes.

The Ag–CuO NCs demonstrated excellent inhibitory activity against *S.aureus* (26±0.53 mm) and *E.coli* (25±0.56 mm) and the fungicidal effects were also examined against *C. albicans* species with maximum ZOI of 20±0.52 mm at 100 mg/mL. Ag–CuO NCs exhibited outstanding DPPH radical scavenging activity with a low IC_{50} value of 35.17µg/mL. Concerning the environmental applications, the Ag–CuO NCs displayed efficient photocatalytic activity against MB dye degradation up to 97% within 120 min. Considering the obtained results, CuO NPs and Ag-CuO NCs fabricated from STPE may be utilized as an efficient antimicrobial agent in treating infectious diseases and antioxidant agent for diseases caused by oxidative stress such as cancer, stroke and diabetes etc. From the photocatalytic studies, the synthesized NCs are found to be promising stable photocatalysts in remediation contaminated water from MB dye under solar irradiation, due to their easy synthetic strategy, unique structure, cost-effectiveness, environmentally friendly starting materials, high catalytic radiation efficiency and rapid contact time.

5.2. Recommendation

Chemists and scientific communities more investigate on phytocapped synthesis on NMs using more on wastes of fruit or vegetable, play great role in circular economy in recycling of wastes in useful fashion and environmental remediation. Furthermore, this study has faced challenge on predicting the morphology and structure of the synthesized NMs due to the lack of advanced characterization methods such as TEM, XPS and EDX. So, further characterization techniques are required to study the surface composition of the synthesized NMs for additional applications.

6. REFERENCE

(1) C Reygaert, W. An Overview of the Antimicrobial Resistance Mechanisms of Bacteria. *AIMS Microbiol.* **2018**, *4* (3), 482–501. https://doi.org/10.3934/microbiol.2018.3.482.

(2) Tao, T.; Zhou, C.; Song, X.; Zhao, Q.; Andersson, P.; Yan, W.; Xu, B. Real-Time Warning and Signal Verification for Infectious Disease Outbreaks Using Syndromic Surveillance System in Rural Jiangxi Province, China. *Online J. Public Health Inform.* **2014**, *6* (1), 2579. https://doi.org/10.5210/ojphi.v6i1.5158.

(3) Huh, A. J.; Kwon, Y. J. "Nanoantibiotics": A New Paradigm for Treating Infectious Diseases Using Nanomaterials in the Antibiotics Resistant Era. *J. Control. Release* **2011**, *156* (2), 128–145. https://doi.org/10.1016/j.jconrel.2011.07.002.

(4) Wang, W.; Li, H.; Lv, J.; Khan, G. J.; Duan, H.; Zhu, J.; Bao, N.; Zhai, K.; Xue, Z. Determination of the Anti-Oxidative Stress Mechanism of Isodon Suzhouensis Leaves by Employing Bioinformatic and Novel Research Technology. *ACS Omega* **2022**. https://doi.org/10.1021/acsomega.2c07913.

(5) Iqbal, J.; Andleeb, A.; Ashraf, H.; Meer, B.; Mehmood, A.; Jan, H.; Zaman, G.; Nadeem, M.; Drouet, S.; Fazal, H.; Giglioli-Guivarc'h, N.; Hano, C.; Abbasi, B. H. Potential Antimicrobial, Antidiabetic, Catalytic, Antioxidant and ROS/RNS Inhibitory Activities of Silybum Marianum Mediated Biosynthesized Copper Oxide Nanoparticles. *RSC Adv.* **2022**, *12* (22), 14069–14083. https://doi.org/10.1039/d2ra01929a.

(6) Sagasta, J. M. *More People, More Food, Worse Water?: A Global Review of Water Pollution from Agriculture*; 2018.

(7) Khan, I.; Saeed, K.; Zekker, I.; Zhang, B.; Hendi, A. H.; Ahmad, A.; Ahmad, S.; Zada, N.; Ahmad, H.; Shah, L. A.; Shah, T.; Khan, I. And Photodegradation. **2022**.

(8) Atri, A.; Echabaane, M.; Bouzidi, A.; Harabi, I.; Soucase, B. M.; Ben Chaâbane, R. Green Synthesis of Copper Oxide Nanoparticles Using Ephedra Alata Plant Extract and a Study of Their Antifungal, Antibacterial Activity and Photocatalytic Performance under Sunlight. *Heliyon* **2023**, *9* (2), 1–16. https://doi.org/10.1016/j.heliyon.2023.e13484.

(9) Shindume L, H.; Zhao, Z.; Wang, N.; Liu, H.; Umar, A.; Zhang, J.; Wu, T.; Guo, Z. Enhanced Photocatalytic Activity of B, N-Codoped TiO 2 by a New Molten Nitrate Process . *J. Nanosci. Nanotechnol.* **2018**, *19* (2), 839–849. https://doi.org/10.1166/jnn.2019.15745.

(10) Ciambelli, P.; La Guardia, G.; Vitale, L. Nanotechnology for Green Materials and Processes. *Stud. Surf. Sci. Catal.* **2019**, *179*, 97–116. https://doi.org/10.1016/B978-0-444-64337-7.00007-0.

(11) Kamila, S.; Venugopal, V. R. Synthesis and Structural Analysis of Different CuO Nano Particles. **2017**, No. November 2016, 133–146. https://doi.org/10.6703/IJASE.2017.14(3).133.

(12) Preethi, D. R. A.; Philominal, A. Antimicrobial and Antiurolithiatic Activities of Pure and

Silver Doped Copper Oxide Nanoparticles Using Moringa Oleifera Leaf Extract on Struvite Urinary Stones. *Appl. Surf. Sci. Adv.* **2022**, *12* (November), 100351. https://doi.org/10.1016/j.apsadv.2022.100351.

(13) Rajendaran, K.; Muthuramalingam, R.; Ayyadurai, S. Green Synthesis of Ag-Mo/CuO Nanoparticles Using Azadirachta Indica Leaf Extracts to Study Its Solar Photocatalytic and Antimicrobial Activities. *Mater. Sci. Semicond. Process.* **2019**, *91* (March 2019), 230–238. https://doi.org/10.1016/j.mssp.2018.11.021.

(14) Adewale, S.; Similoluwa, A.; Adekunle, F.; Kolawole, A. Heliyon Green Synthesis of Copper Oxide Nanoparticles for Biomedical Application and Environmental Remediation. *Heliyon* **2020**, *6* (July), e04508. https://doi.org/10.1016/j.heliyon.2020.e04508.

(15) Rigano, M. M.; De Guzman, G.; Walmsley, A. M.; Frusciante, L.; Barone, A. Production of Pharmaceutical Proteins in Solanaceae Food Crops. *Int. J. Mol. Sci.* **2013**, *14* (2), 2753–2773. https://doi.org/10.3390/ijms14022753.

(16) Gebrechristos, H. Y.; Ma, X.; Xiao, F.; He, Y.; Zheng, S.; Oyungerel, G.; Chen, W. Potato Peel Extracts as an Antimicrobial and Potential Antioxidant in Active Edible Film. *Food Sci. Nutr.* **2020**, *8* (12), 6338–6345. https://doi.org/10.1002/fsn3.1119.

(17) Elemike, E. E.; Onwudiwe, D. C.; Ogeleka, D. F.; Mbonu, J. I. Phyto-Assisted Preparation of Ag and Ag–CuO Nanoparticles Using Aqueous Extracts of Mimosa Pigra and Their Catalytic Activities in the Degradation of Some Common Pollutants. *J. Inorg. Organomet. Polym. Mater.* **2019**, *29* (5), 1798–1806. https://doi.org/10.1007/s10904-019-01142-y.

(18) Roy, K.; Ghosh, C. K. Environmental and Biological Applications of Nanoparticles. *Nanotechnology* **2017**, 147–169. https://doi.org/10.1201/9781315116730-8.

(19) Jadhav, M. S.; Kulkarni, S.; Raikar, P.; Barretto, D. A.; Vootla, S. K.; Raikar, U. S. Green Biosynthesis of CuO & Ag-CuO Nanoparticles from Malus Domestica Leaf Extract and Evaluation of Antibacterial, Antioxidant and DNA Cleavage Activities. *New J. Chem.* **2018**, *42* (1), 204–213. https://doi.org/10.1039/c7nj02977b.

(20) Arumai Selvan, D. S.; Kumar, R. S.; Murugesan, S.; Shobana, S.; Rahiman, A. K. Antidiabetic Activity of Phytosynthesized Ag/CuO Nanocomposites Using Murraya Koenigii and Zingiber Officinale Extracts. *J. Drug Deliv. Sci. Technol.* **2022**, *67* (xxxx), 102838. https://doi.org/10.1016/j.jddst.2021.102838.

(21) Mohamed, D. S.; El-Baky, R. M. A.; Sandle, T.; Mandour, S. A.; Ahmed, E. F. Antimicrobial Activity of Silver-Treated Bacteria against Other Multi-Drug Resistant Pathogens in Their Environment. *Antibiotics* **2020**, *9* (4). https://doi.org/10.3390/antibiotics9040181.

(22) Sharma, J.; Sharma, S.; Soni, V. Classification and Impact of Synthetic Textile Dyes on Aquatic Flora: A Review. *Reg. Stud. Mar. Sci.* **2021**, *45*. https://doi.org/10.1016/j.rsma.2021.101802.

(23) Uwishema, O.; Okereke, M.; Onyeaka, H.; Hasan, M. M.; Donatus, D.; Martin, Z.;

Oluwatomisin, L. A.; Mhanna, M.; Olumide, A. O.; Sun, J.; Adanur, I. Threats and Outbreaks of Cholera in Africa amidst COVID-19 Pandemic: A Double Burden on Africa's Health Systems. *Trop. Med. Health* **2021**, *49* (1). https://doi.org/10.1186/s41182-021-00376-2.

(24) Letta, T. T.; Belay, D. B.; Ali, E. A. Determining Factors Associated with Cholera Disease in Ethiopia Using Bayesian Hierarchical Modeling. *BMC Public Health* **2022**, *22* (1), 1–10. https://doi.org/10.1186/s12889-022-14153-1.

(25) Pulingam, T.; Parumasivam, T.; Gazzali, A. M.; Sulaiman, A. M.; Chee, J. Y.; Lakshmanan, M.; Chin, C. F.; Sudesh, K. Antimicrobial Resistance: Prevalence, Economic Burden, Mechanisms of Resistance and Strategies to Overcome. *Eur. J. Pharm. Sci.* **2022**, *170*, 106103. https://doi.org/10.1016/j.ejps.2021.106103.

(26) Musoke, D.; Namata, C.; Lubega, G. B.; Niyongabo, F.; Gonza, J.; Chidziwisano, K.; Nalinya, S.; Nuwematsiko, R.; Morse, T. The Role of Environmental Health in Preventing Antimicrobial Resistance in Low- and Middle-Income Countries. *Environmental Health and Preventive Medicine*. BioMed Central Ltd December 1, 2021. https://doi.org/10.1186/s12199-021-01023-2.

(27) Singh, A.; Kukreti, R.; Saso, L.; Kukreti, S. Oxidative Stress: A Key Modulator in Neurodegenerative Diseases. *Molecules* **2019**, *24* (8), 1–20. https://doi.org/10.3390/molecules24081583.

(28) Gupta, D. Methods for Determination of Antioxidant Capacity: A Review. *Int. J. Pharm. Sci. Res.* **2015**, *6* (2), 546–566. https://doi.org/10.13040/IJPSR.0975-8232.6(2).546-66.

(29) Khalil, I.; Yehye, W. A.; Etxeberria, A. E.; Alhadi, A. A.; Dezfooli, S. M.; Julkapli, N. B. M.; Basirun, W. J.; Seyfoddin, A. Nanoantioxidants: Recent Trends in Antioxidant Delivery Applications. *Antioxidants* **2020**, *9* (1). https://doi.org/10.3390/antiox9010024.

(30) Agensi, A.; Tibyangye, J.; Tamale, A.; Agwu, E.; Amongi, C. Contamination Potentials of Household Water Handling and Storage Practices in Kirundo Subcounty, Kisoro District, Uganda. *J. Environ. Public Health* **2019**, *2019*. https://doi.org/10.1155/2019/7932193.

(31) Malik, A.; Grohmann, E. *Environmental Protection Strategies for Sustainable Development*; 2012. https://doi.org/10.1007/978-94-007-1591-2.

(32) Jeevanandam, J.; Barhoum, A.; Chan, Y. S.; Dufresne, A.; Danquah, M. K. Review on Nanoparticles and Nanostructured Materials: History, Sources, Toxicity and Regulations. *Beilstein J. Nanotechnol.* **2018**, *9* (1), 1050–1074. https://doi.org/10.3762/bjnano.9.98.

(33) Bayda, S.; Adeel, M.; Tuccinardi, T.; Cordani, M.; Rizzolio, F. The History of Nanoscience and Nanotechnology: From Chemical-Physical Applications to Nanomedicine. *Molecules* **2020**, *25* (1), 1–15. https://doi.org/10.3390/molecules25010112.

(34) Tshireletso, P.; Ateba, C. N.; Fayemi, O. E. Spectroscopic and Antibacterial Properties of CuONPs from Orange, Lemon and Tangerine Peel Extracts: Potential for Combating

Bacterial Resistance. *Molecules* **2021**, *26* (3). https://doi.org/10.3390/molecules26030586.

(35) Meghana, S.; Kabra, P.; Chakraborty, S.; Padmavathy, N. Understanding the Pathway of Antibacterial Activity of Copper Oxide Nanoparticles. *RSC Adv.* **2015**, *5* (16), 12293–12299. https://doi.org/10.1039/c4ra12163e.

(36) Hasan, I.; Shekhar, C.; Sharfan, I. I. Bin; Khan, R. A.; Alsalme, A. Ecofriendly Green Synthesis of the ZnO-Doped CuO @ Alg Bionanocomposite for E Ffi Cient Oxidative Degradation of p - Nitrophenol. **2020**. https://doi.org/10.1021/acsomega.0c04917.

(37) Naz, S.; Gul, A.; Zia, M.; Javed, R. Synthesis, Biomedical Applications, and Toxicity of CuO Nanoparticles. *Appl. Microbiol. Biotechnol.* **2023**, *107* (4), 1039–1061. https://doi.org/10.1007/s00253-023-12364-z.

(38) Titus, D.; James Jebaseelan Samuel, E.; Roopan, S. M. *Nanoparticle Characterization Techniques*; Elsevier Inc., 2018. https://doi.org/10.1016/B978-0-08-102579-6.00012-5.

(39) Khan, F.; Shariq, M.; Asif, M.; Siddiqui, M. A.; Malan, P.; Ahmad, F. Green Nanotechnology: Plant-Mediated Nanoparticle Synthesis and Application. *Nanomaterials* **2022**, *12* (4). https://doi.org/10.3390/nano12040673.

(40) Alhalili, Z. Green Synthesis of Copper Oxide Nanoparticles CuO NPs from Eucalyptus Globoulus Leaf Extract: Adsorption and Design of Experiments. *Arab. J. Chem.* **2022**, *15* (5), 103739. https://doi.org/10.1016/j.arabjc.2022.103739.

(41) Chakraborty, N.; Banerjee, J.; Chakraborty, P.; Banerjee, A.; Chanda, S.; Ray, K.; Acharya, K.; Sarkar, J. Green Synthesis of Copper/Copper Oxide Nanoparticles and Their Applications: A Review. *Green Chem. Lett. Rev.* **2022**, *15* (1), 185–213. https://doi.org/10.1080/17518253.2022.2025916.

(42) Friedman, M.; Huang, V.; Quiambao, Q.; Noritake, S.; Liu, J.; Kwon, O.; Chintalapati, S.; Young, J.; Levin, C. E.; Tam, C.; Cheng, L. W.; Land, K. M. Potato Peels and Their Bioactive Glycoalkaloids and Phenolic Compounds Inhibit the Growth of Pathogenic Trichomonads. **2018**, 8–13. https://doi.org/10.1021/acs.jafc.8b01726.

(43) Helal, M. M.; Adawy, T. A. E.-; Beltagy, A. E. E.-; Bedawey, A. A. E.-; Youssef, S. M. Evaluation of Potato Peel Extract As a Source of Antioxidant and Antimicrobial Substances. *Menoufia J. Food Dairy Sci.* **2020**, *5* (6), 79–90. https://doi.org/10.21608/mjfds.2020.171473.

(44) Ncube, A.; Mtetwa, S.; Bukhari, M.; Fiorentino, G.; Passaro, R. Circular Economy and Green Chemistry: The Need for Radical Innovative Approaches in the Design for New Products. *Energies* **2023**, *16* (4), 1–21. https://doi.org/10.3390/en16041752.

(45) Javed, A.; Ahmad, A.; Tahir, A.; Shabbir, U.; Nouman, M.; Hameed, A. Potato Peel Waste—Its Nutraceutical, Industrial and Biotechnological Applacations. *AIMS Agric. Food* **2019**, *4* (3), 807–823. https://doi.org/10.3934/agrfood.2019.3.807.

(46) Shinde, R. S.; More, R. A.; Adole, V. A.; Koli, P. B.; Pawar, T. B.; Jagdale, B. S.; Desale, B. S.; Sarnikar, Y. P. Design, Fabrication, Antitubercular, Antibacterial, Antifungal and

Antioxidant Study of Silver Doped ZnO and CuO Nano Candidates: A Comparative Pharmacological Study. *Curr. Res. Green Sustain. Chem.* **2021**, *4*. https://doi.org/10.1016/j.crgsc.2021.100138.

(47) Ashour, A. H.; El-Batal, A. I.; Maksoud, M. I. A. A.; El-Sayyad, G. S.; Labib, S.; Abdeltwab, E.; El-Okr, M. M. Antimicrobial Activity of Metal-Substituted Cobalt Ferrite Nanoparticles Synthesized by Sol–Gel Technique. *Particuology* **2018**, *40*, 141–151. https://doi.org/10.1016/j.partic.2017.12.001.

(48) Silva, B. L. da; Abuçafy, M. P.; Manaia, E. B.; Junior, J. A. O.; Chiari-Andréo, B. G.; Pietro, R. C. L. R.; Chiavacci, L. A. Relationship between Structure and Antimicrobial Activity of Zinc Oxide Nanoparticles: An Overview. *Int. J. Nanomedicine* **2019**, *14*, 9395–9410. https://doi.org/10.2147/IJN.S216204.

(49) Gerasimova, E.; Gazizullina, E.; Kolbaczkaya, S.; Ivanova, A. The Novel Potentiometric Approach to Antioxidant Capacity Assay Based on the Reaction with Stable Radical 2,2′-Diphenyl-1-Picrylhydrazyl. *Antioxidants* **2022**, *11* (10). https://doi.org/10.3390/antiox11101974.

(50) Goswami, M. Enhancement of Photocatalytic Activity of Synthesized Cobalt Doped Zinc Oxide Nanoparticles under Visible Light Irradiation. *Opt. Mater. (Amst).* **2020**, *109* (August), 110400. https://doi.org/10.1016/j.optmat.2020.110400.

(51) Kaliva, M.; Vamvakaki, M. *Nanomaterials Characterization*; Elsevier Inc., 2020. https://doi.org/10.1016/B978-0-12-816806-6.00017-0.

(52) Mulvaney, P. Surface Plasmon Spectroscopy of Nanosized Metal Particles. *Langmuir* **1996**, *12* (3), 788–800. https://doi.org/10.1021/la9502711.

(53) Taha, M.; Hassan, M.; Essa, S.; Tartor, Y. Use of Fourier Transform Infrared Spectroscopy (FTIR) Spectroscopy for Rapid and Accurate Identification of Yeasts Isolated from Human and Animals. *Int. J. Vet. Sci. Med.* **2013**, *1* (1), 15–20. https://doi.org/10.1016/j.ijvsm.2013.03.001.

(54) Britain, G. The General Principles of Scanning Electron Microscopy. *Philos. Trans. R. Soc. London. B, Biol. Sci.* **1971**, *261* (837), 45–50. https://doi.org/10.1098/rstb.1971.0035.

(55) Chauhan, A. Powder XRD Technique and Its Applications in Science and Technology. *J. Anal. Bioanal. Tech.* **2014**, *5* (6). https://doi.org/10.4172/2155-9872.1000212.

(56) El-Desouky, N.; Shoueir, K.; El-Mehasseb, I.; El-Kemary, M. Synthesis of Silver Nanoparticles Using Bio Valorization Coffee Waste Extract: Photocatalytic Flow-Rate Performance, Antibacterial Activity, and Electrochemical Investigation. *Biomass Convers. Biorefinery* **2022**, No. 0123456789. https://doi.org/10.1007/s13399-021-02256-5.

(57) Firisa, S. G.; Muleta, G. G.; Yimer, A. A. Synthesis of Nickel Oxide Nanoparticles and Copper-Doped Nickel Oxide Nanocomposites Using Phytolacca Dodecandra L'Herit Leaf Extract and Evaluation of Its Antioxidant and Photocatalytic Activities. *ACS Omega* **2022**. https://doi.org/10.1021/acsomega.2c04042.

(58) Angeloni, G.; Masella, P.; Guerrini, L.; Innocenti, M.; Bellumori, M.; Parenti, A. Application of a Screening Design to Recover Phytochemicals from Spent Coffee Grounds. *Food Bioprod. Process.* **2019**, *118*, 50–57. https://doi.org/10.1016/j.fbp.2019.08.017.

(59) Andrade, C.; Perestrelo, R.; Câmara, J. S. Bioactive Compounds and Antioxidant Activity from Spent Coffee Grounds as a Powerful Approach for Its Valorization. *Molecules* **2022**, *27* (21), 7504. https://doi.org/10.3390/molecules27217504.

(60) Iqbal, E.; Salim, K. A.; Lim, L. B. L. Phytochemical Screening, Total Phenolics and Antioxidant Activities of Bark and Leaf Extracts of Goniothalamus Velutinus (Airy Shaw) from Brunei Darussalam. *J. King Saud Univ. - Sci.* **2015**, *27* (3), 224–232. https://doi.org/10.1016/j.jksus.2015.02.003.

(61) Budlayan, M. L. M.; Patricio, J. N.; Arco, S. D.; Capangpangan, R. Y.; Alguno, A. C. Effects of Precursor Concentration on the Properties of Magnetic Iron Oxide Nanoparticles Synthesized Using Brown Seaweed (Sargassum Crassifolium) Extract. *Mater. Today Proc.* **2020**, *46* (xxxx), 1608–1612. https://doi.org/10.1016/j.matpr.2020.07.251.

(62) Chen, M. N.; Chan, C. F.; Huang, S. L.; Lin, Y. S. Green Biosynthesis of Gold Nanoparticles Using Chenopodium Formosanum Shell Extract and Analysis of the Particles' Antibacterial Properties. *J. Sci. Food Agric.* **2019**, *99* (7), 3693–3702. https://doi.org/10.1002/jsfa.9600.

(63) Lenders, J. J. M.; Mirabello, G.; Sommerdijk, N. A. J. M. Bioinspired Magnetite Synthesis via Solid Precursor Phases. *Chem. Sci.* **2016**, *7* (9), 5624–5634. https://doi.org/10.1039/c6sc00523c.

(64) Patra, J. K.; Baek, K. H. Green Nanobiotechnology: Factors Affecting Synthesis and Characterization Techniques. *J. Nanomater.* **2014**, *2014*. https://doi.org/10.1155/2014/417305.

(65) Darroudi, M.; Ahmad, M. Bin; Zamiri, R.; Zak, A. K.; Abdullah, A. H.; Ibrahim, N. A. Time-Dependent Effect in Green Synthesis of Silver Nanoparticles. *Int. J. Nanomedicine* **2011**, *6* (1), 677–681. https://doi.org/10.2147/IJN.S17669.

(66) Preethi, D. R. A.; Philominal, A. Green Synthesis of Pure and Silver Doped Copper Oxide Nanoparticles Using Moringa Oleifera Leaf Extract. *Mater. Lett. X* **2022**, *13*, 100122. https://doi.org/10.1016/j.mlblux.2022.100122.

(67) Cheng, Y.; Wang, M.; Fang, C.; Wei, Y.; Chen, J.; Zhang, J. Variability and Improvement of Optical and Antimicrobial Performances for CQDs/Mesoporous SiO2/Ag NPs Composites via in Situ Synthesis. *Green Process. Synth.* **2021**, *10* (1), 403–411. https://doi.org/10.1515/gps-2021-0035.

(68) Vijayakumar, M.; Priya, K.; Nancy, F. T.; Noorlidah, A.; Ahmed, A. B. A. Biosynthesis, Characterisation and Anti-Bacterial Effect of Plant-Mediated Silver Nanoparticles Using Artemisia Nilagirica. *Ind. Crops Prod.* **2013**, *41* (1), 235–240.

https://doi.org/10.1016/j.indcrop.2012.04.017.

(69) Alamier, W. M.; Oteef, M. D. Y.; Bakry, A. M.; Hasan, N.; Ismail, K. S.; Awad, F. S. Green Synthesis of Silver Nanoparticles Using Acacia Ehrenbergiana Plant Cortex Extract for Efficient Removal of Rhodamine B Cationic Dye from Wastewater and the Evaluation of Antimicrobial Activity. *ACS Omega* **2023**, *8* (21), 18901–18914. https://doi.org/10.1021/acsomega.3c01292.

(70) Helal, M. M.; El-Adawy, T. A.; El-Beltagy, A. E.; El-Bedawey, A. .; Youssef, S. M. Evaluation of Potato Peel Extract As a Source of Antioxidant and Antimicrobial Substances. *Menoufia J. Food Dairy Sci.* **2020**, *5* (8), 79–90. https://doi.org/10.21608/mjfds.2020.113467.

(71) Sampaio, S. L.; Petropoulos, S. A.; Dias, M. I.; Pereira, C.; Calhelha, R. C.; Fernandes, Â.; Leme, C. M. M.; Alexopoulos, A.; Santos-Buelga, C.; Ferreira, I. C. F. R.; Barros, L. Phenolic Composition and Cell-Based Biological Activities of Ten Coloured Potato Peels (Solanum Tuberosum L.). *Food Chem.* **2021**, *363* (June). https://doi.org/10.1016/j.foodchem.2021.130360.

(72) Peddi, P.; Ptsrk, P. R.; Rani, N. U.; Tulasi, S. L. Green Synthesis, Characterization, Antioxidant, Antibacterial, and Photocatalytic Activity of Suaeda Maritima (L.) Dumort Aqueous Extract-Mediated Copper Oxide Nanoparticles. *J. Genet. Eng. Biotechnol.* **2021**, *19* (1). https://doi.org/10.1186/s43141-021-00229-9.

(73) Melkamu, W. W. Green Synthesis of Copper Oxide Nanoparticles Using Leaf Extract of Justicia Schimperiana and Their Antibacterial Activity. **2022**, 1–24.

(74) Letchumanan, D.; Sok, S. P. M.; Ibrahim, S.; Nagoor, N. H.; Arshad, N. M. Plant-Based Biosynthesis of Copper/Copper Oxide Nanoparticles: An Update on Their Applications in Biomedicine, Mechanisms, and Toxicity. *Biomolecules* **2021**, *11* (4). https://doi.org/10.3390/biom11040564.

(75) Yazdani, S.; Daneshkhah, A.; Diwate, A.; Patel, H.; Smith, J.; Reul, O.; Cheng, R.; Izadian, A.; Hajrasouliha, A. R. Model for Gold Nanoparticle Synthesis: Effect of PH and Reaction Time. *ACS Omega* **2021**, *6* (26), 16847–16853. https://doi.org/10.1021/acsomega.1c01418.

(76) Akanda, M. R.; Al-amin, M.; Mele, M. A.; Shuva, Z. M.; Hossain, M. B.; Islam, T.; Hasan, M. M.; Ema, U. H. Parameters Optimization of Fe3O4 NPs Synthesis by Tamarindus Indica Leaf Extract Possessing Both Peroxidase as Well as Excellent Dye Removal Activity. *Heliyon* **2023**, *9* (6), e16699. https://doi.org/10.1016/j.heliyon.2023.e16699.

(77) Gaba, S.; Rai, A. K.; Varma, A.; Prasad, R.; Goel, A. Biocontrol Potential of Mycogenic Copper Oxide Nanoparticles against Alternaria Brassicae. *Front. Chem.* **2022**, *10* (August), 1–18. https://doi.org/10.3389/fchem.2022.966396.

(78) Selvanathan, V.; Aminuzzaman, M.; Tey, L. H.; Razali, S. A.; Althubeiti, K.; Alkhammash, H. I.; Guha, S. K.; Ogawa, S.; Watanabe, A.; Shahiduzzaman, M.;

Akhtaruzzaman, M. Muntingia Calabura Leaves Mediated Green Synthesis of Cuo Nanorods: Exploiting Phytochemicals for Unique Morphology. *Materials (Basel).* **2021**, *14* (21), 1–12. https://doi.org/10.3390/ma14216379.

(79) Udayabhanu; Nethravathi, P. C.; Pavan Kumar, M. A.; Suresh, D.; Lingaraju, K.; Rajanaika, H.; Nagabhushana, H.; Sharma, S. C. Tinospora Cordifolia Mediated Facile Green Synthesis of Cupric Oxide Nanoparticles and Their Photocatalytic, Antioxidant and Antibacterial Properties. *Mater. Sci. Semicond. Process.* **2015**, *33* (April 2021), 81–88. https://doi.org/10.1016/j.mssp.2015.01.034.

(80) Javid-Naderi, M. J.; Sabouri, Z.; Jalili, A.; Zarrinfar, H.; Samarghandian, S.; Darroudi, M. Green Synthesis of Copper Oxide Nanoparticles Using Okra (Abelmoschus Esculentus) Fruit Extract and Assessment of Their Cytotoxicity and Photocatalytic Applications. *Environ. Technol. Innov.* **2023**, *32*, 103300. https://doi.org/10.1016/j.eti.2023.103300.

(81) Buazar, F.; Bavi, M.; Kroushawi, F.; Halvani, M.; Khaledi-Nasab, A.; Hossieni, S. A. Potato Extract as Reducing Agent and Stabiliser in a Facile Green One-Step Synthesis of ZnO Nanoparticles. *J. Exp. Nanosci.* **2016**, *11* (3), 175–184. https://doi.org/10.1080/17458080.2015.1039610.

(82) Rodríguez-Martínez, B.; Gullón, B.; Yáñez, R. Identification and Recovery of Valuable Bioactive Compounds from Potato Peels: A Comprehensive Review. *Antioxidants* **2021**, *10* (10), 1–18. https://doi.org/10.3390/antiox10101630.

(83) Phang, Y. K.; Aminuzzaman, M.; Akhtaruzzaman, M.; Muhammad, G.; Ogawa, S.; Watanabe, A.; Tey, L. H. Green Synthesis and Characterization of CuO Nanoparticles Derived from Papaya Peel Extract for the Photocatalytic Degradation of Palm Oil Mill Effluent (POME). *Sustain.* **2021**, *13* (2), 1–15. https://doi.org/10.3390/su13020796.

(84) Uma, B.; Anantharaju, K. S.; Surendra, B. S.; Gurushantha, K.; More, S. S.; Meena, S.; Hemavathi, B.; Murthy, H. C. A. Influence of Ag on the Structural, Electrochemical, Antibacterial, and Photocatalytic Performance of the (CuO-Cu2O)Cu Nanocomposite. *ACS Omega* **2023**, *8* (11), 9947–9961. https://doi.org/10.1021/acsomega.2c07124.

(85) Yang, H.; Ren, Y. yu; Wang, T.; Wang, C. Preparation and Antibacterial Activities of Ag/Ag+/Ag3+ Nanoparticle Composites Made by Pomegranate (Punica Granatum) Rind Extract. *Results Phys.* **2016**, *6*, 299–304. https://doi.org/10.1016/j.rinp.2016.05.012.

(86) Kumar, P.; Chandra Mathpal, M.; Prakash, J.; Viljoen, B. C.; Roos, W. D.; Swart, H. C. Band Gap Tailoring of Cauliflower-Shaped CuO Nanostructures by Zn Doping for Antibacterial Applications. *J. Alloys Compd.* **2020**, *832*, 154968. https://doi.org/10.1016/j.jallcom.2020.154968.

(87) Menazea, A. A.; Mostafa, A. M. Ag Doped CuO Thin Film Prepared via Pulsed Laser Deposition for 4-Nitrophenol Degradation. *J. Environ. Chem. Eng.* **2020**, *8* (5), 104104. https://doi.org/10.1016/j.jece.2020.104104.

(88) Singh, J.; Dutta, T.; Kim, K. H.; Rawat, M.; Samddar, P.; Kumar, P. "Green" Synthesis of Metals and Their Oxide Nanoparticles: Applications for Environmental Remediation. *J.*

Nanobiotechnology **2018**, *16* (1), 1–24. https://doi.org/10.1186/s12951-018-0408-4.

(89) Aien, J.; Khan, A. A.; Haq, S.; Khan, A. R.; Elmnasri, K.; Ben Ali, M.; AL-Harbi, M. S.; Alghonaim, M. I.; Alsalamah, S. A.; Qurtam, A. A.; Boufahja, F.; Hedfi, A.; Dellali, M. Antibacterial, Antioxidant and Physicochemical Properties of Pipper Nigram Aided Copper Oxide Nanoparticles. *Crystals* **2023**, *13* (2). https://doi.org/10.3390/cryst13020330.

(90) More, P. R.; Pandit, S.; Filippis, A. De; Franci, G.; Mijakovic, I.; Galdiero, M. Silver Nanoparticles : Bactericidal and Mechanistic Approach against Drug Resistant Pathogens. **2023**.

(91) Parvathiraja, C.; Shailajha, S. Bioproduction of CuO and Ag/CuO Heterogeneous Photocatalysis-Photocatalytic Dye Degradation and Biological Activities. *Appl. Nanosci.* **2021**, *11* (4), 1411–1425. https://doi.org/10.1007/s13204-021-01743-5.

(92) Topal Canbaz, G.; Keskin, Z. S.; Yokuş, A.; Aslan, R. Biofabrication of Copper Oxide Nanoparticles Using Solanum Tuberosum L. Var. Vitelotte: Characterization, Antioxidant and Antimicrobial Activity. *Chem. Pap.* **2023**, *77* (8), 4277–4284. https://doi.org/10.1007/s11696-023-02776-6.

(93) Velsankar, K.; Aswin Kumara, R. M.; Preethi, R.; Muthulakshmi, V.; Sudhahar, S. Green Synthesis of CuO Nanoparticles via Allium Sativum Extract and Its Characterizations on Antimicrobial, Antioxidant, Antilarvicidal Activities. *J. Environ. Chem. Eng.* **2020**, *8* (5), 104123. https://doi.org/10.1016/j.jece.2020.104123.

(94) Nandhakumar, E.; Priya, P.; Selvakumar, P.; Vaishnavi, E.; Sasikumar, A.; Senthilkumar, N. One Step Hydrothermal Green Approach of CuO/Ag Nanocomposites: Analysis of Structural, Biological Activities. *Mater. Res. Express* **2019**, *6* (9). https://doi.org/10.1088/2053-1591/ab2eb9.

(95) El-Ansary, A. E.; Omran, A. A. A.; Mohamed, H. I.; El-Mahdy, O. M. Green Synthesized Silver Nanoparticles Mediated by Fusarium Nygamai Isolate AJTYC1: Characterizations, Antioxidant, Antimicrobial, Anticancer, and Photocatalytic Activities and Cytogenetic Effects. *Environ. Sci. Pollut. Res.* **2023**, *30* (45), 100477–100499. https://doi.org/10.1007/s11356-023-29414-8.

(96) Tam, K. T.; Thanh, D. Van; Van, H. T.; Mai, N. T. P.; Hai, C. T.; Phuong, T. M.; Xuan, N. T.; Nguyen, V.-T. Green Synthesis of Silver Nanoparticles Using Extract of Disporopsis Longifolia for Photocatalytic Degradation of Methylene Blue . *Am. J. Environ. Sci.* **2022**, *18* (5), 116–124. https://doi.org/10.3844/ajessp.2022.116.124.

(97) Dulta, K.; Ko, G.; Chauhan, P.; Jasrotia, R.; Chauhan, P. K.; Ighalo, J. O. Multifunctional CuO Nanoparticles with Enhanced Photocatalytic Dye Degradation and Antibacterial Activity. **2022**.

(98) Mahlaule-Glory, L. M.; Mapetla, S.; Makofane, A.; Mathipa, M. M.; Hintsho-Mbita, N. C. Biosynthesis of Iron Oxide Nanoparticles for the Degradation of Methylene Blue Dye, Sulfisoxazole Antibiotic and Removal of Bacteria from Real Water. *Heliyon* **2022**, *8* (9),

e10536. https://doi.org/10.1016/j.heliyon.2022.e10536.

(99) Oladoye, P. O.; Ajiboye, T. O.; Omotola, E. O.; Oyewola, O. J. Methylene Blue Dye: Toxicity and Potential Elimination Technology from Wastewater. *Results Eng.* **2022**, *16* (August), 100678. https://doi.org/10.1016/j.rineng.2022.100678.

(100) Munir, M.; Nazar, M. F.; Zafar, M. N.; Zubair, M.; Ashfaq, M.; Hosseini-Bandegharaei, A.; Khan, S. U. D.; Ahmad, A. Effective Adsorptive Removal of Methylene Blue from Water by Didodecyldimethylammonium Bromide-Modified Brown Clay. *ACS Omega* **2020**, *5* (27), 16711–16721. https://doi.org/10.1021/acsomega.0c01613.

(101) Avis, A.; Babu, T.; Antony, R. Green Synthesis of Silver Doped Nano Metal Oxides of Zinc & Copper for Antibacterial Properties, Adsorption, Catalytic Hydrogenation & Photodegradation of Aromatics. *Biochem. Pharmacol.* **2018**. https://doi.org/10.1016/j.jece.2018.102840.

(102) Baste, Y.; Jadhav, V.; Roy, A.; Alghamdi, S.; Abbas, M.; Algethami, J. S. Polyol Synthesis of Ag-Doped Copper Oxide Nanoparticles as a Methylene Blue-Degrading Agent. **2023**, 1–14.

(103) Amina, M.; Al Musayeib, N. M.; Alterary, S.; El-Tohamy, M. F.; Alhwaiti, S. A. Advanced Polymeric Metal/Metal Oxide Bionanocomposite Using Seaweed Laurencia Dendroidea Extract for Antiprotozoal, Anticancer, and Photocatalytic Applications. *PeerJ* **2023**, *11*. https://doi.org/10.7717/peerj.15004.

(104) Anjum, F.; Shaban, M.; Ismail, M.; Gul, S.; Bakhsh, E. M.; Khan, M. A.; Sharafat, U.; Khan, S. B.; Khan, M. I. Novel Synthesis of CuO/GO Nanocomposites and Their Photocatalytic Potential in the Degradation of Hazardous Industrial Effluents. *ACS Omega* **2023**, *8* (20), 17667–17681. https://doi.org/10.1021/acsomega.3c00129.

7.LIST OF APPENDICES

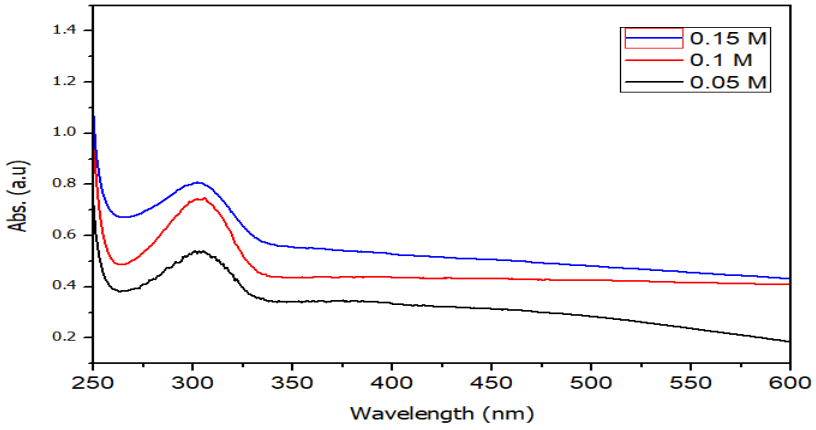

Appendix 1. Uv-vis spectral results of concentration of precursor salt optimization

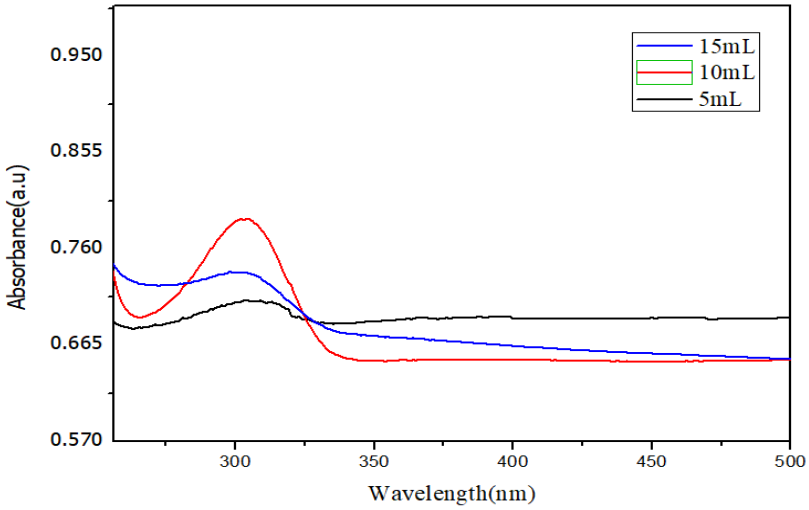

Appendix 2.Uv-vis spectral result of extract optimization

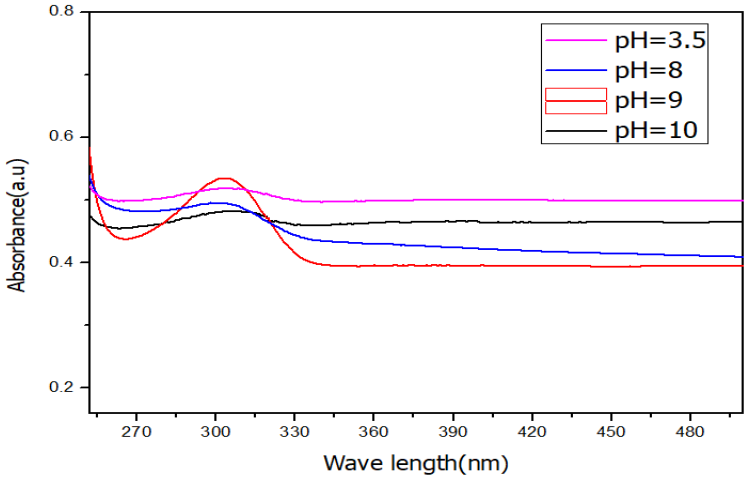

Appendix 3 . Uv-vis spectral result of pH optimization

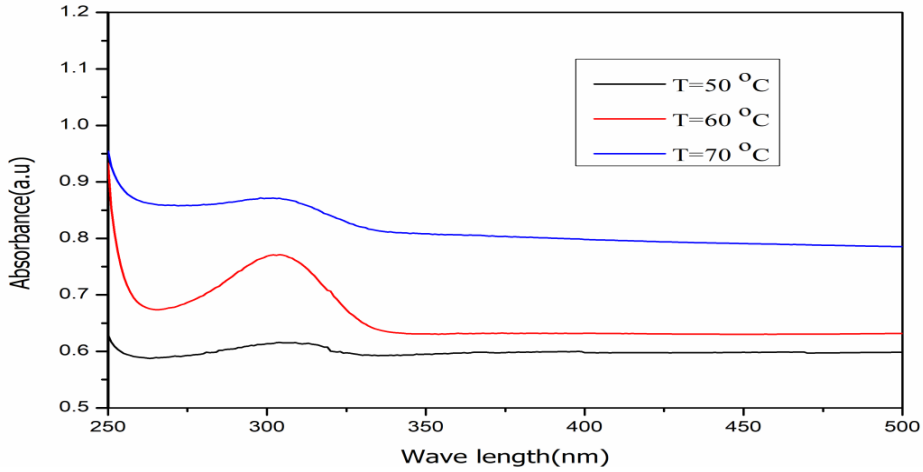

Appendix 4.Uv-vis spectral result of temperature optimization

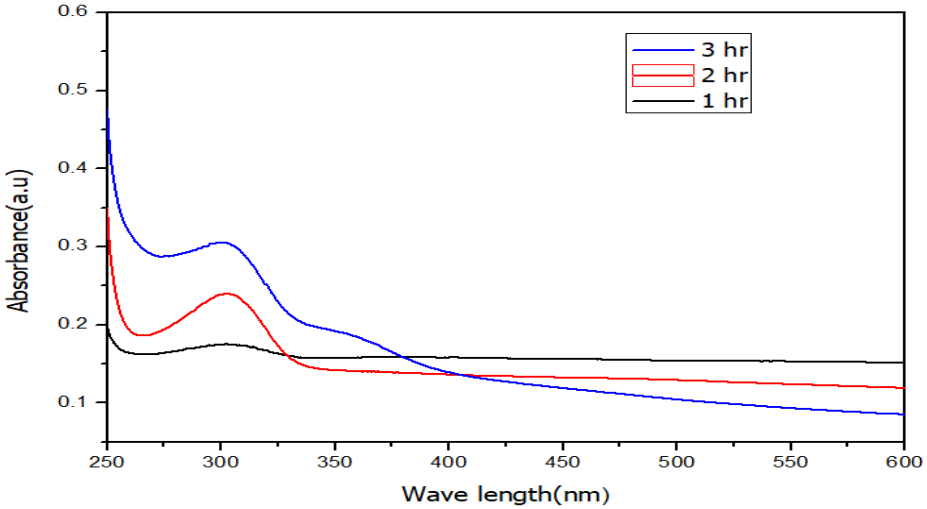

Appendix 5. Uv-vis spectral result of time optimization

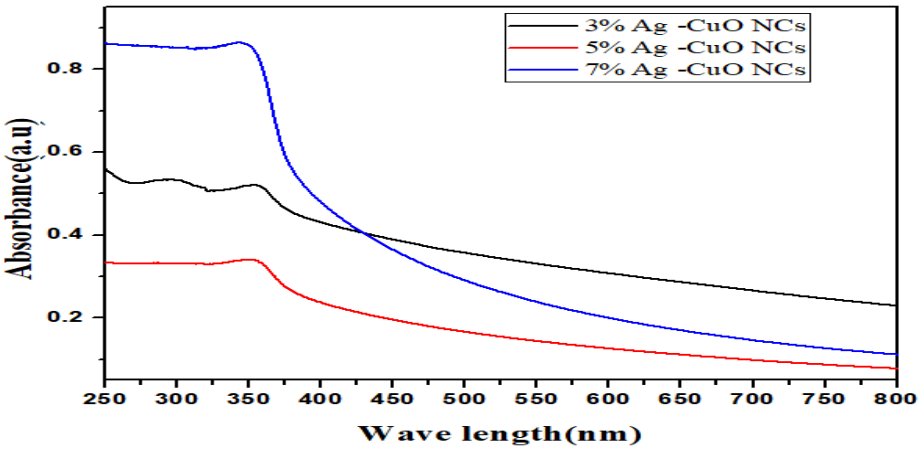

Appendix 6. Optimization of amount of dopant (Ag)

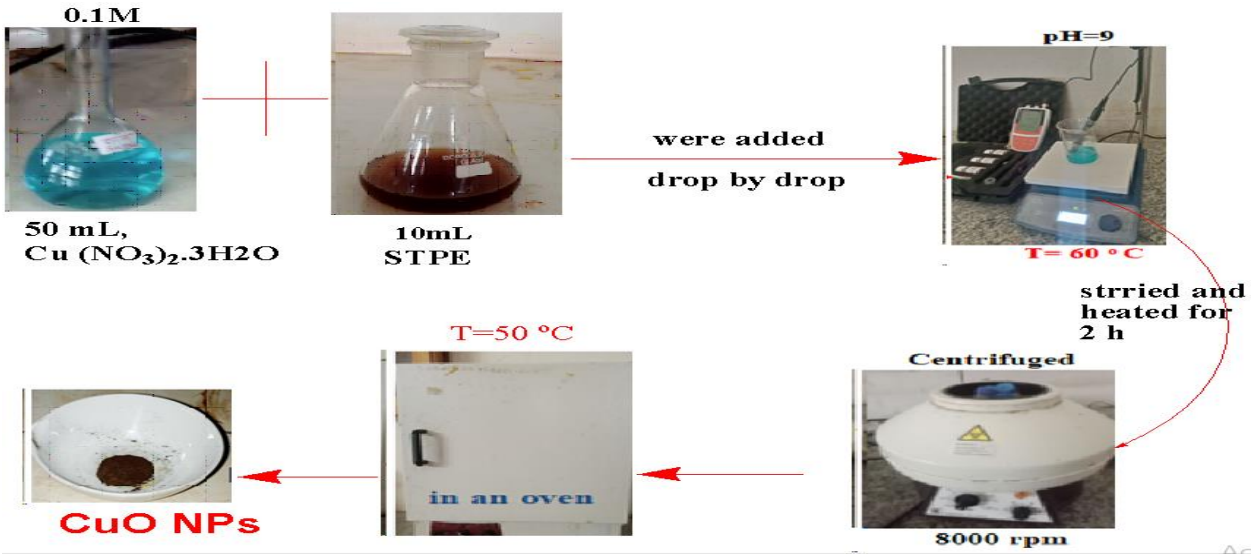

Appendix 7.synthesis of CuO NPs

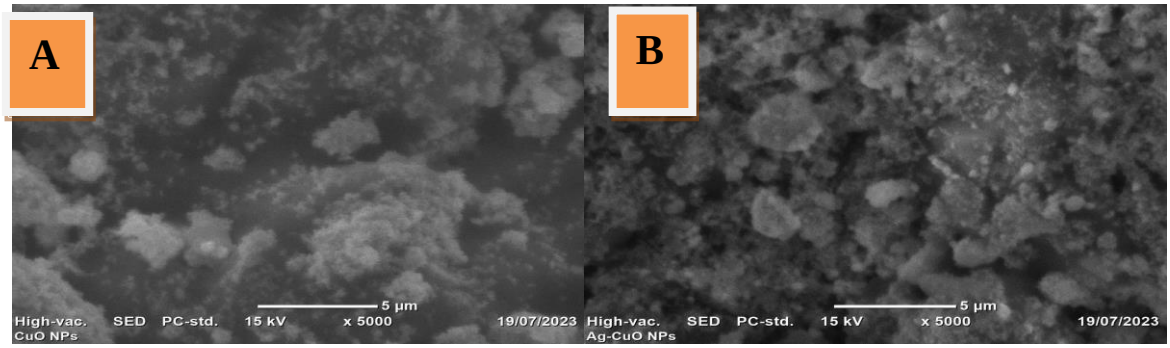

Appendix 8. (A) SEM images of CuO NPs and,(B) Ag-CuO NCs at magnification of 5000x.

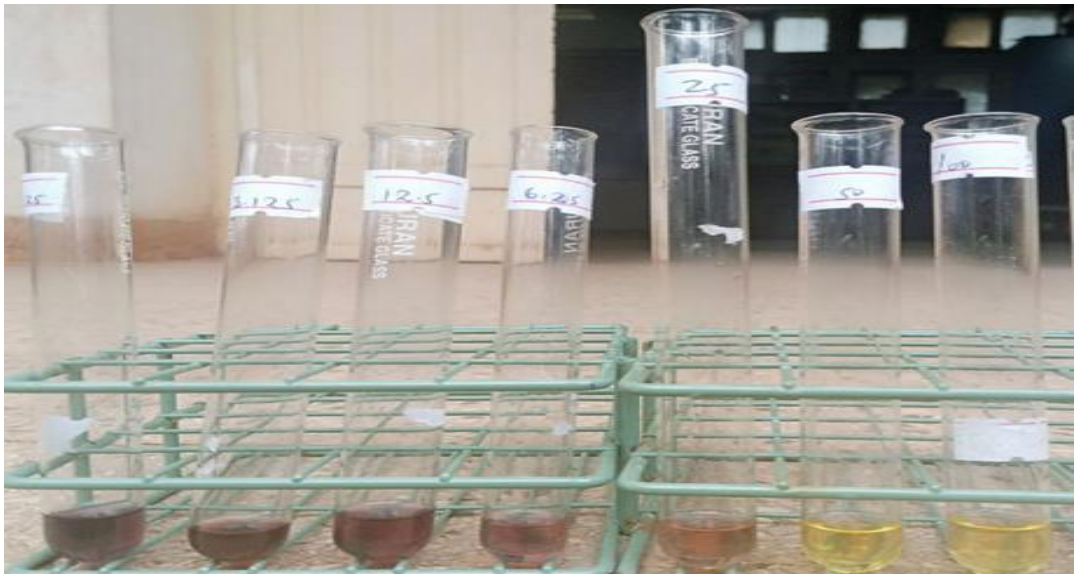

Appendix 9. Antioxidant activity test concentration by DPPH assay.

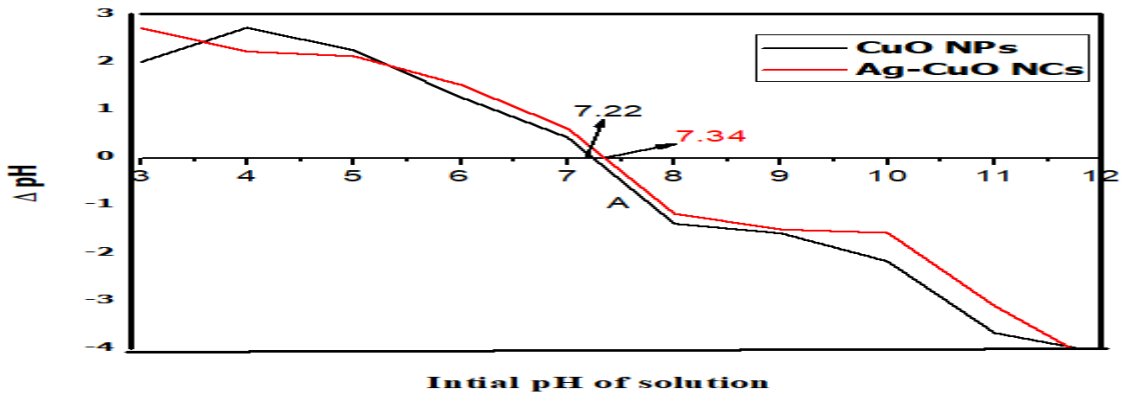

Appendix 10. Graph of point zero charge of CuO NPs and Ag-CuO NCs

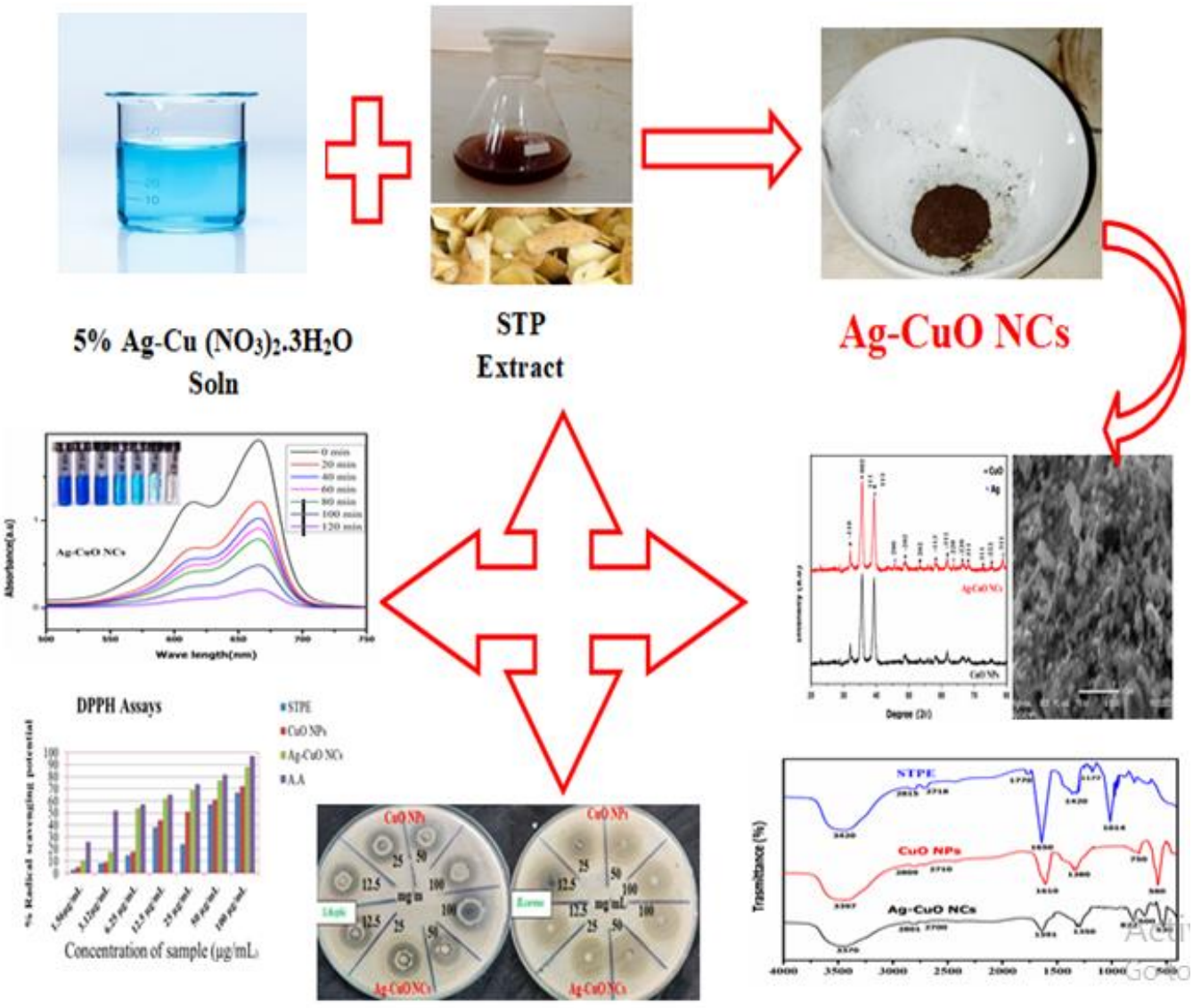

Appendix 11. Graphical abstract representations of synthesis, characterization and application of Ag-CuO NCs